Evaluation of quick clay failures and the impact of climate change on slope stability

ACEX11 Bachelor thesis

Group 37

Kiana Farmanesh

Emma Gummesson

William Ryberg

Arvid Sandberg

CHALMERS UNIVERSITY OF TECHNOLOGY

Gothenburg, Sweden 2024

Bachelor's thesis 2024

Evaluation of quick clay failures and the impact of climate change on slope stability

KIANA FARMANESH, EMMA GUMMESSON, WILLIAM RYBERG, ARVID SANDBERG

Department of Architecture and Civil Engineering
Division of Geology and geotechnics
Chalmers University of Technology
Gothenburg, Sweden 2024

Evaluation of quick clay failures and the impact of climate change on slope stability

© KIANA FARMANESH, EMMA GUMMESSON, WILLIAM RYBERG, ARVID SANDBERG.

Supervisor: Ayman Abed, Senior Lecturer, Geology and Geotechnics, Architecture and Civil Engineering

Bachelor's Thesis 2024 Department of Architecture and Civil Engineering
Division of Geology and geotechnics
Chalmers University of Technology
SE-412 96 Gothenburg
Telephone +46 31 772 1000

Cover: The aftermaths of landslide in Stenungsund 2023 Credits: Per Pixel Petersson with premission

Abstract

This bachelor's thesis investigates the phenomenon of quick clay failure, focusing on the triggering factors behind landslides in Western Sweden and Norway. The aim was to map a pattern in historical events and with retained knowledge about quick clay and scenarios in climate change estimate future slope stability. To understand the triggering factors an investigation was conducted ranging from the structure of bedrock to the chemistry of clay particles.

Water is one of the main factors that contribute to the formation of quick clay landslides and the characteristics of specific clay types. New precipitation patterns risk increased infiltration and flow in the soil which raises the importance of efficient risk mitigation strategies against slope failures. Alterations in hydrology were investigated, and how they affect parameters defining the strength and capacity to resist movements in the slope. Climate scenarios were used to forecast the influence of climate change on the global water cycle and consequently, its impact on future landslide occurrences.

Historical factors of four landslides were compiled and analyzed. Multiple simulations of the Tuve landslide were conducted in Geostudio with analysis in Seep/W and Slope/w for three different sections. The understanding of quick clay properties, coupled with simulation results, led to the conclusion that the catastrophic landslide in Tuve in 1977 was a translational progressive landslide originating from Tuve kyrkväg. The extensive scale of the landslide was due to the initial slide disrupting the clay, transforming it into a liquefied state, thereby reducing the shear strength to zero causing the rest of the area to collapse. The behavior of quick clay is unpredictable and difficult to estimate the extent of a slide due to the possibility of a serial failure post an initial perturbation. The discussion highlights the importance of mitigating strategies and early indicators of potential hazards.

Keywords: Tuve, Landslide, Quick clay, Saftey factor, Slope failure

Contents

1 Introduction

Quick clay is a specific type of clay primarily found in the western part of Sweden and in extensive regions of Norway and Canada. Quick clay is typically formed from clay deposited in saltwater under glacial marine conditions near a melting ice sheet [1]. Due to the regression of the ice sheet landmass rises above the sea level, leaving clay with a high concentration of salt above today's sea level. Normally, quick clay is relatively stable, but when exposed to a disturbance the shear strength in the structure can decrease close to zero, leading to landslides with significant spatial extent which can be a disaster in residential and densely populated areas and to critical infrastructure.

The high sensitivity of quick clay which indicate the relationship between undrained shear strength and the disturbed sample is primarily connected to processes that occur after the clay has been deposited on the sea floor. The key process in the scenario is the leaching of salt ions due to infiltration of precipitation, artesian pressure and diffusion of salt [1]. This concentration of ions acts as binding links between clay particles in combined aggregates. The reason behind the unfavorable properties in quick clay is the lack of ability to reform these aggregates after destruction.

Examples of the destructive impact quick clay landslides have had in Sweden include the E6 failure in September 2023, as well as incidents in Tuve and Småröd in 1977 and 2006, respectively, resulting in injuries and property damage. Additionally, it is shown that human activities are a common cause of historical landslides in Sweden [2]. The combination of human-made perturbations with the behavior of quick clay is clearly a potential risk of initiating extensive landslides. To prevent such disasters in the future, it is crucial to enhance knowledge and awareness of the risks within the engineering industry including its response to future developments and climate change.

The increasing trends in development and climate change indicate a potential rise in the frequency of landslides [3]. This emphasizes the importance of having a well-established foundation of data for construction and urban planning decisions. This report was conducted to provide a deeper understanding of quick clay and what triggers landslides in areas with quick clay. Global warming will continue to increase in the near future according to almost all the scenarios and pathway models created by the Intergovernmental Panel on Climate Change (IPPC) sixth assessment [4]. Continued global warming is forecasted to intensify the dynamics of the global water cycle, including variability in precipitation patterns worldwide. As temperatures rise, the evaporation of water from oceans, lakes, and land surfaces accelerates, contributing to increased moisture in the atmosphere. This surplus moisture can result in more frequent and intense precipitation events across various regions of the globe.

With climate change threatening to increase the heavy precipitation, the risk of landslides follows. To prevent such disasters in the future, it is crucial to enhance knowledge and awareness of the risks within the engineering industry including its response to future developments and climate change. Through our work, we hope to contribute to the understanding of quick clay and its connections to landslides, as well as how the climate factor accelerates the process.

1.1 Purpose

The project aims to comprehend the diverse factors that trigger quick clay landslides. A model of the Tuve landslide is utilized to conduct an in-depth analysis of the contributing factors to a landslide in quick clay. Future factors such as soil conditions, topography, precipitation, and human influence are factors that we will investigate in the literature part of the report to understand how these interact and contribute to the destabilization of the ground. The findings of this analysis will contribute to an enhanced understanding of the mechanism behind landslides in quick clay. They may thus inform future preventive measures and risk management strategies for similar areas.

1.2 Scope

Quick clay generally requires a disturbance in the structure to trigger a landslide. The aim is to map the causes behind historical landslides. In addition simulations in Geostudio will be utilized to map the critical disturbances needed to trigger slope failure.

We have constructed the following diverse research questions as guidelines during this project.

- What are the defining characteristics of quick clay in geotechnical and geological contexts?
- What factors trigger landslides, specifically quick clay landslides?
- What were the triggering factors in specific cases, i.e., Tuve?
- What common triggers are observed in the previous landslide cases?
- How will climate change impact quick clay failure in the future, specifically in the west of Sweden?
- How is the movement in the ground connected to landslides?

1.3 Delimitations

This report aims to highlight and map what triggers quick clay failures with a brief discussion around the economic and political aspects of landslides. Simulations of quick clay failure in the future caused by climate change is restricted to year 2100 because that is the current estimations provided by IPCC. Because of uncertainties in the variables this factor will not be applied as a boundary condition in the Geostudio modeling but will instead be used to support the obtained results. Chosen geometries will only address landslides in areas with clay that has similar properties deposited in marine environments.

1.4 Methodology

The report contains useful information gathered from literature documents regarding historical landslides in the bordering area of Gothenburg. The information was mainly collected from different technical reports and articles provided by geological institutions i.e. the Geological Survey of Sweden and the Swedish Geotechnical Institute. Satellite images from inSAR were investigated to examine movements in the ground prior the landslide in Stenungsund. To investigate the causes behind the sudden landslides, the work includes a comprehensive analysis of the geotechnical properties and parameters of the clay such as sensitivity, shear strength, and the structure of the clay deposits in marine environments. This data worked as the foundation to investigate future complications of quick clay with regard to climate change.

Data provided by the IPCC, Intergovernmental Panel on Climate Change, was applied in theory to estimate the extent of geotechnical-related failures due to climate change and variation in future precipitation as well as temperature [5].

1.4.1 Geostudio

Computer analyses in Geostudio was conducted to complement the data provided in the literature studies. The focus was on analyzing the topography in Tuve and calculating safety factors with different methods of triggering slides. The model was constructed based on data such as earth layering and groundwater table provided by the Geotechnical Institution of Sweden and in situ investigations. Within Geostudio, boundary conditions were applied in Seep/W to build a transient flow after which calculations with fluctuating slope stability in Slope/W was conducted.

SEEP/W

A numerical model represents a mathematical emulation of an actual physical phenomenon. SEEP/W serves as such a model, capable of accurately simulating the movement of water through a medium. Finite element numerical methods rely on dividing a continuous entity into smaller segments, detailing the behavior or characteristics of each segment, and assembling them to portray the overall behavior of the entity. This segmentation process is called meshing, with the individual segments referred to as finite elements. There are two different analyses used in SEEP/W. They are steady-state and transient flow.

The first step was to define the geometry and the initial boundary conditions in terms of water to generate flow paths. The next step in our analysis was to include transient water conditions due to applied fluctuations on the surface with fluxes to represent infiltration and change in the water head.

SLOPE/W

Slope/W was used to simulate the stability of the slopes giving a safety factor as output. The slope/W simulations were done with the output data and geometry from seep/W. This data in combination with soil strength data collected from the respective areas makes up the foundation of the stability analysis conducted in slope/W.

With the aid of Geostudio, an investigation of the Tuve landslide was conducted with the geometry from the documents provided. The data was collected from the geotechnical reports of SGI [6]. Three different sections A-A, B-B, and C-C were analyzed, comparing the initial stability in each section with resulting stability after applied infiltration of water in the soil. The main focus of the analysis was to investigate how infiltration and increased flow in the underlying friction layer were going to impact the safety factor. Different methods were used to simulate the slide surface and in this case, a fully specified method was utilized to obtain the slide which occurred in the frictional layer. The chapter 'Simulations in Geostudio', provides a comprehensive elucidation of our simulation methodologies.

2 Prerequisite in local geology and behavior of quick clay

Quick clay is most commonly found in the western part of Sweden [7], which is the same region in Sweden where cases of landslides will be investigated in this report. To understand the occurrence of quick clay it is important to understand the geology and topography in these areas [1]. In the following chapter, the regional geology and prerequisites of the formation of quick clay will be discussed.

2.1 Clay deposited in water

Quick clay is generally deposited in saline water under glaciomarine conditions near a melting ice sheet [7]. Thus quick clay occurs in areas with large ice sheets during the latest glaciation. When the ice sheets began to retreat these areas were covered with water and the most fine-grained glacial sediments were deposited in the most significant depth forming clay.

Since the last ice age, the Baltic Sea has experienced alternating conditions due to the complex interaction between the melting of the ice sheet, land uplift, and changes in the global sea level [7]. Stages with alternating brackish-marine and freshwater conditions have existed under different periods. In the western part of Sweden, clays have been deposited under mainly marine conditions, e.g. in Halland, Bohuslän, Dalsland, and lower-lying areas around Värnen.

2.2 Distinguishing areas

There are different methods and factors to examine while distinguishing areas with prerequisites for quick clay.

In the report "Quick clay in Sweden" Rankka et al. describe different characteristics of areas more prone to forming quick clay. Figure 1 shows how to distinguish regions with prerequisites for quick clay [1].

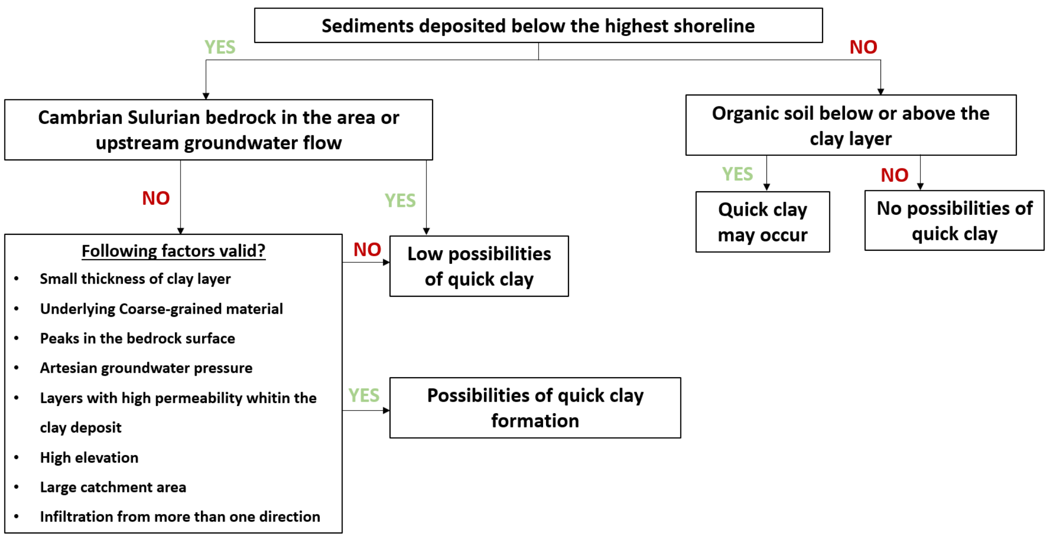

Figure 1: Flowchart for finding areas with prerequisites of quick clay. Author's own image based on material in [1]

Sediments deposited below the highest shoreline and organic soils
By examining the highest sea level for an area one can find where clay has been deposited in sea water where most of the quick clay has been formed [1]. The large deposits are found at elevations below approximately 80 percent of the level of the highest shoreline. Furthermore, quick clay is more prone to areas in contact with organic soils.

Cambrain-Silurian bedrock in the area or upstream the groundwater flow
The possibilities for clay to have quick properties are limited if it has been leached in hard groundwater [1]. Hard groundwater is often found around areas where the bedrock is of limestone formed during the Cambrian, Ordovician, and Silurian periods. It is important to note that quick clay has been found near limestone areas in Sweden, and one has to examine the groundwater flow to evaluate the likelihood of leaching with hard groundwater.

Small thickness of clay layer
The leaching process is prolonged in low-permeable soil and the time for the leaching process to reduce the salt content to a sufficiently low level depends on the thickness

of the sediment layer [1]. This causes quick clay to be more prone to areas where the deposits are thinner and close to permeable water-conducting layers.

Underlying Coarse-grained material

Groundwater can infiltrate through coarse-grained soil beneath the clay deposit [1]. The amount of water depends on the thickness of the soil layer, along with the permeability and if the soil is in direct contact with rainwater or water-conducting fractures in the bedrock.

Often a layer of till is created between the layer of clay deposit and bedrock, which through in-situ test, can be considered as water-conducting. The areas where thicker layers of till can be discovered are found at locations of extensive ice-marginal deposits. These formations can be found in a wide band across Sweden and most of the quick clay formations exist in the same areas.

Peaks in the bedrock surface

Elevated points in the underlying bedrock beneath the soil layer lead to a focal point of groundwater outflow, resulting in heightened leaching and the potential formation of quick clay [1]. Unexplained minor depressions in the ground surface are indicators of subsurface quick clay formation.

Artesian groundwater pressure

Areas with artesian groundwater pressure are more prone to quick clay formation compared with hydrostatic conditions [1]. This is due to the three different types of leaching processes (rainwater percolating through the deposit, an upward hydraulic gradient, and diffusion) that are strongly affected by the hydraulic gradient. These conditions exist where thick water-conducting layers are found below the clay deposits, in sloping areas where the water from higher ground leads to thick layers of water-conducting materials beneath the clay deposits, and where the bedrock has many fracture zones.

A similar effect may occur if there is a downward gradient in pore water and the surface run-off is insufficient or aquifers surmount clay layers.

Layers with high permeability within the clay deposit

Geotechnical and geological investigations can help find areas where permeable layers, such as silt and sand, are embedded in the clay deposits and in contact with water [1]. These areas are more prone to leaching and the high permeability depends on variations during sedimentation. Rankka et al. state some examples: "... i.e. in the distance to the ice front, the material carried and deposited by the streaming water, the flow velocity, the topography, the sea water level and on the situation after the ice regression (post-glacial sediments). Major geological events causing formations of distinctly different layers are temporary re-advancements of the ice front during colder periods, transgression periods with rising sea levels, the breaking through of ice-dammed lakes, etc." So places to examine are areas relevant to these characteristics.

High elevation
Sediments at higher levels have been exposed to the leaching process over a longer period [1]. If one compares lower and higher elevated areas with all other prerequisites being equal, the highest area is more likely to have quick clay. This is except for clays located above the elevation of the highest shoreline.

Catchment areas and infiltration from more than one direction
Topographical maps can show the extent of the catchment area in which all precipitation is led to the clay deposit [1]. The greater the catchment area and annual precipitation are the greater the possibilities of leaching, thus the prerequisites for the formation of clay. The topography map can also show the occurrence of bare hills in multiple directions which increases the possibility of water infiltration and leaching.

2.3 Geology of Tuve and Stenungsund

Tuve is one of the older cases of landslide we investigate in this report, and Stenungsund is the most recent. Investigating these according to figure 1 reveals similarities.

The geology of Tuve consists of a major peak to the north and minor elevation variations to the south, characterized by red feldspar, granite, amphibolite, and diabase rock formations [8]. Pronounced fracture zones with high water conductivity exist. Surrounding areas have moraine-covered mountain regions and clay layers extending up slopes, interspersed with sandy and silty sediments. In Stenungsund, tonalite and granite gneissic bedrock prevail [9] . Ground levels vary from +35 m near the river to +100 m in mountainous regions. The area is connected to the Norum river and Ucklum road in the north, bounded by mountainous terrain in the south and east, and by Road 170 in the west. Materials in landslide areas consist of post-glacial sand or dry clayey soil overlying clay resting on a frictional layer on bedrock, with clay layers varying from 2 m to 40 m, thickest centrally.

The clay in Tuve and Stenungsund is likely deposited in seawater as both areas lies below the highest coastline [10]. Thinner layers of sedimentary clay are present in certain parts of both of the areas, with the bedrock non-consistent of limestone. Artesian groundwater pressure and layers with high permeability exist within the clay sediments of the Tuve area. Therefore, as expected, conditions conducive to quick clay formation are present in both regions.

2.4 Fundamentals of quick clay behavior

To analyze how and why landslides occur, an understanding of the chemical composition of the soil is needed. Clay consists of particles smaller than 0.002 millimeters [11]. These particles are minerals that have been formed from chemical and physical weathering creating a skeleton structure with pores containing air and fluids [12].

Quick clay generates behavior following failure or disturbance, diverging from typical soft clays. These clays transform in consistency, transitioning from stable solid structure to liquefied states. To meet Swedish classification criteria as quick clay certain conditions must be met. The remoulded undrained shear strength must be less than 0.4 kPa, and the sensitivity, maximum shear strength divided by remoulded undrained shear strength must exceed 50 [12]. Regions such as Finland, Norway, Sweden, and Canada harbor quick clays, a commonality among them being their coverage by the continental ice sheet during the last glacial period and the landlift post-glacial melting.

2.4.1 Structure of quick clay

The arrangement of the particles depends on the fact that the flat side is usually negatively charged and the edges are positively charged. This is due to minerals on the longer sides being replaced by ions with lower valence numbers leading to an attracting force forming and maintaining the structure of particles. Clay is always deposited in slow-running water as the particles are small and easily disturbed in moving water.

Significant clusters are generated as a consequence of the elevated presence of ions in the ocean, prompting particles to draw near due to attractive forces. Clay sedimentation occurs without distinct organization or orientation, facilitating the settling of small clusters into a more compact formation compared to larger ones. Consequently, the substantial clusters, which settle in high-salinity water, yield a larger and denser structure, whereas those in freshwater yield a more porous one [13]. This discrepancy results in larger inter-cluster pores for clays deposited in saltwater seen in figure 2, thereby increasing porosity and enabling the clay to retain significant water levels.

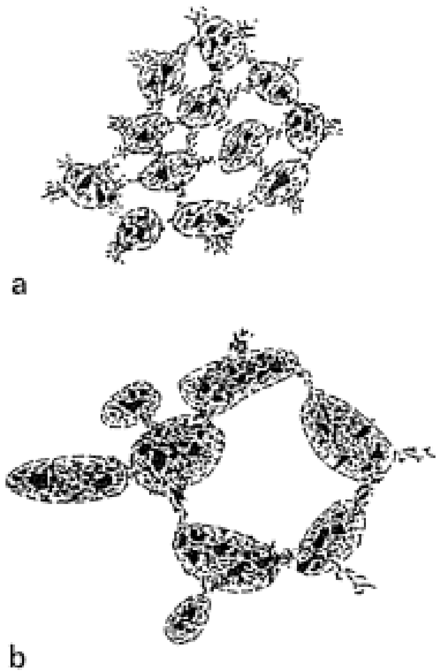

Figure 2: Pictures of aggregate structure in clay. a) Fresh water and b) Sea water [14]

2.4.2 Properties of quick clay

Above the groundwater level, water can become entrapped in isolated pockets with artesian pressure conditions [15]. Capillary rise is caused by the surface tension between a liquid and the adjacent materials [16]. If the clay was deposited in salt water or brackish water, salt minerals can still be present in the pores as ions dissolved in water. Due to the small size of the pores in clay, the water has a lot of surface area to attract to, therefore the capillary rise is high. However, the rising of the water is slow due to the low permeability of clay.

For clay deposited in saltwater leaching of salt ions is the main cause of weakening the structure of mineral grains, this is due to the fact that the salt ions have an integral part in the structure of the mineral clusters. Leaching occurs more rapidly when clay is near a permeable layer capable of transporting water. Essentially, there are three distinct leaching processes. Precipitation including rain and snow filtering down through the deposit, water moving upward through the deposit created by artesian pressure, and the migration of salts toward areas with decreased ion concentrations through diffusion. The water typically has a lower concentration of salt ions, thereby facilitating diffusion away from the clay.

Lowering the charge of the flat sides of the mineral elements creates negative charged surface that attracts cations [12]. If the clay has high water content these cations can dissolve in the water creating a charged layer around the grain, instead of precipitating onto the clay grain. If the concentration of ions is low this layer takes up more space as shown in figure 3. This layer result in a repelling force that prohibits the clay minerals from returning to their original state when the clay has been disturbed.

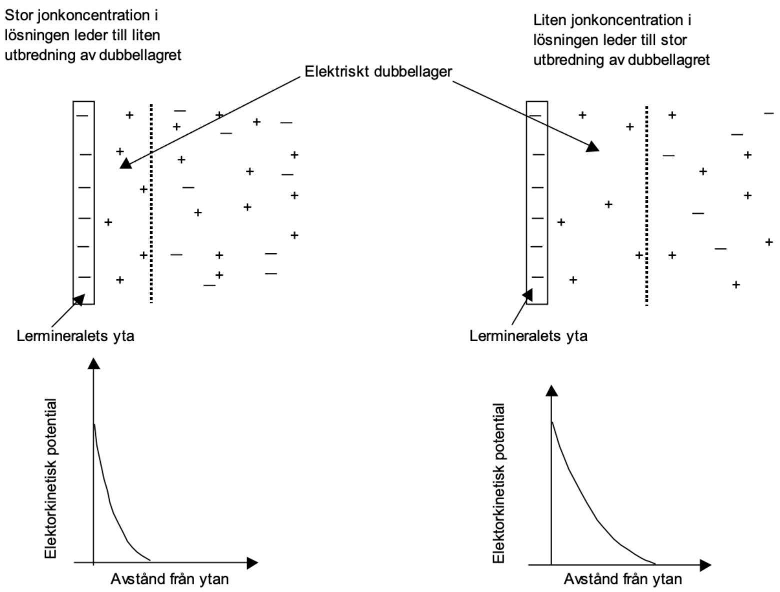

Figure 3: Illustration of charged double layer [12]

Organic matter, such as roots, releases hydrogen ions (H^+) which replace ions in the mineral's crystal lattice. Due to differences in size and charge, these hydrogen ions do not seamlessly fit into the lattice, thereby weakening its structure and making it more prone to weathering [12]. The weathering makes the clay more sensitive to further erosion.

The disturbance required for clay to transform into quick clay depends on the properties of the clay and the environment where it was deposited. The disturbance can be generated through vibrations from construction, additional loading, or movement in the soil. The magnitude of these disturbances required to reduce the shear strength varies depending on the strength of the chemical bonds in the clay. The alteration in the chemical cohesion of the clay can be influenced by several different processes. When the clay is disturbed the structure and pores collapse, the decrease in pore volume from the collapse lowers the liquid limit of the clay. The lower liquid limit causes the clay particles to float free in the water creating a liquid clay with a shear strength close to zero.

All these factors contribute to the large difference in remoulded and undisturbed clay which leads to high sensitivity of the clay thereby classifying it as quick.

2.5 Failure mechanism

Landslides are commonly associated with large-scale quick clay slides in Scandinavia and Canada. In general slides in sensitive clay are characterized by having large dimensions that can fail in different stages with high velocity [17]. The movement of a slope is a complex matter. However, some differences make it possible to separate different slides from one another. A common way to describe the events happening in a slope failure is to divide into i) pre-failure, ii) failure, iii) post-failure [18]. The process can be explained with four different failure types. They are single rotational slides, multiple retrogressive slides (flows), translational progressive landslides, and spreads [19]. In previous cases a combination of different slides are common. The landslide in Tuve 1977 is an example of a widespread landslide with a huge spatial extent in terms of a progressive landslide [2].

2.5.1 Multiple retrogressive slides

Multiple retrogressive landslides are expected to originate from an initial triggering slide with a completely remoulded structure flowing out of the surface leaving an unstable edge [20]. Retrogressive slides are triggered by an initial loss of support at the foot of the slope creating a pattern that is bound to repeat itself [2]. When the support on the passive side is removed, another slope failure can easily be triggered and work its way up until the retrogressive behavior has stopped.

When evaluating a slope and the impact of a disturbance it is important to separate the long-term and short-term effects. According to Bernander, how you should deal with retrogressive investigations can be translated into three phases [2].

1. **The long-term in situ shear stress and earth pressure conditions.**

   It is important to evaluate the existing in situ stresses to asses the risk destabilizing actions play on the stability.

2. **The disturbance condition**

   2a - Disturbance created by short-term effects like excavation and loading. Typically associated with human activities.

   2b - Long time effect. Disturbances in this category can be long-term chemical and mechanical processes in the soil such as the leaching of ions and erosion in the passive zone.

3. **Dynamic disintegration phase**

   Retrogressive landslides typically do not reach a stable state of equilibrium due to inadequate passive earth pressure resistance at the base of the slope. Instead, the process of dynamic disintegration of the soil mass is prone to unpredictable characteristics.

2.5.2 Translational progressive landslide or downward progressive failures

Translational landslides generally occur in gently inclined slopes and are characterized by a zone of subsidence at the head of the slope and a zone with heaving of the earth at the lower part [20]. Typically, for such a slides to occur, a local disturbance is required which then progresses through a surface and causes a global progressive slip surface since the peak shear resistance is exceeded along it. The formation of this slide looks like a single slide body in simplification. However, Bernander [21] claims that the event cannot be seen as one because of the following serial behavior.

1. **In situ stage**

   The established long-time shear stresses and earth pressure.

2. **The impact of disturbance force**

   A perturbing force that can trigger an initial slide.

3. **Dynamic redistribution of forces**

   This phase represents a redistribution of stresses, deformation, and earth pressures where the unbalanced steep parts of the slope are transmitted downwards to the foot of the slope.

4. **Transition of possible equilibrium**

   In this stage, a final transitory equilibrium is reached before the failure is developed.

5. **Final breakdown**

   This is the moment the final breakdown happens with a specified slide surface with the heaving of the passive zone.

2.5.3 Spreads

According to Cruden and Varnes [19], spreads occur due to the extension and displacement of the soil mass above the failure surface, leading to the formation of horsts and grabens that settle into the underlying remolded material, creating the shear zone. Horsts are characterized by blocks of relatively intact clay, often with a sharp wedge pointing upwards, while grabens typically have a flat, horizontal top surface [20]. These geomorphologic features are crucial in distinguishing spreads from other retrogressive landslides. This type is commonly found in Canada and is not frequent in Sweden. However, examples of such movements in Sweden include the Sköttorp landslide [22]. The series of horsts and grabens could arise from the subsidence of a graben, resulting in an unstable surface that is then pushed downslope by another graben, thereby creating a new horst. The potential existence of a weak layer, facilitating the movement of blocks above it, might explain the observed retrogression.

3 History of landslides cause and consequences

As explained in the previous chapters, quick clay is highly sensitive to vibrations and disturbances leading to extensive landslides and following disasters [23]. The goal is to avoid these disasters as an engineer. However, quick clay is a difficult matter and things can easily get out of control with quick clay deposits making the process even more challenging.

Our understanding of quick clay and landslide occurrences is continuously evolving, with the recorded history of landslides in Sweden dating back to approximately 1150 [24]. Despite the long history of landslide cases in Sweden, it was not until the Tuve landslide in 1977 that the phenomena of "quick clay" and "landslides" were comprehensively examined [25]. The incident acted as an eye-opener, reshaping society's perception of risks of landslides.

Due to the Tuve landslide devastating consequences, the Ministry of Housing and Urban Development assigned the Swedish Geotechnical Institute (SGI) to do an examination of the geotechnical conditions surrounding the landslide [25]. Around the same time projects aiming to map quick clay presence were funded by for instance the Swedish Civil Contingencies Agency (MSB) and Geological Survey of Sweden (SGU) [26].

With an increase in investigations into the phenomenon of quick clay landslides over time, knowledge has expanded. With a broad foundation of information encompassing both theoretical knowledge of quick clay and its management, as well as detailed mapping documentation, engineering tasks rely heavily on comprehensive data, minimizing the risk of catastrophic events. The majority of this foundation was achieved by analyzing and understanding the past events, which this thesis is partly based on. To comprehend quick clay landslides the thesis is going to analyze different cases such as Tuve (1977), Småröd (2006), Stenungsund (2023) and Gjerdrum (2021).

3.1 Tuve

Tuve landslide took place November 30, 1977 shortly after 4 PM, in a duration of 5 minutes. A total area of 27 hectares was affected with a maximum displacement of 800 meters in the direction of landslide and a maximum width of 600 meters. The incident lead to 9 lost lives and 151 properties and buildings were either completely destroyed or severely damaged [25]. The investigations were done through the years directly after the event where the final investigation were presented in 1984 in four separate reports by the Swedish Geotechnical Institute (SGI) [25].

3.1.1 Challenges through the investigation

The investigation that followed the Tuve landslide reveals the limited knowledge about the contributing causes behind a landslide. The lack of detailed geotechnical documentation prior to the event added an additional challenge to the investigation [25].

As a result of the insufficient documentation, the soil strength could not be determined to the desired extent [27]. In order to continue with the investigation reasonable assumptions were taken regarding strength parameters and pore pressure. These assumptions were partly based on the existing geotechnical documentation before the Tuve landslide and partly on later field investigations in close approximation to the landslide area. It is also taken into account that these assumptions and investigations may not fully represent the real parameters and conditions of the undisturbed soil layers.

Due to the large scale of the landslide, naturally, the attention were paid to examine large progressive slides [27]. These kind of large-scaled landslides typically starts at the baseline of the slope or another vulnerable area, such as an eroded stream slope.

Looking for the cause of the event, the stability of various potential sliding surfaces in the landslide area was examined. Consequently, it is determined that the stability for Tuve Kyrkväg was low [27].

3.1.2 Kvilledalen before the landslide

Figure 4: Picture taken from Tuve before the landslide occurred, showing areas topography and landslides area marked in the figure [25]

Kvilledalen where the landslide occurred (figure 4), is located a few meters above the sea level at its lowest point. The area resembles a small valley with mountains covering north and south. Through this valley a small stream was followed. In the specific area between the new Tuvevägen and Tuve Kyrkväg, there was a slope with the steepest sections east of Tuve Kyrkväg. The slope inclination in these areas were about 1:5 and steepest as 1:3. The stream had eroded a ravine and it was culverted and discharged into Kvilledalen down into Kvillebäcken [25].

The erosion of the culverted ravine was due to exploitation of Tuve. The actual exploring started 1957 with constructing two-story townhouses along Tångvägen leading to a closely clustered neighborhood in Tuve and Tångelunds area. Throught these urbanizations the stormwater was handeled by connecting it to the stream. This led to an increased water flow in the stream and furthurmore culvert installation in the previous eroded ravine was the solution to handle the increased flow [25].

3.1.3 Environmental conditions

Previous weeks prior to the event there was substantial precipitation [8]. The rainfall during the November of 1977 marked the highest recorded levels since the culverting of the stream [25]. The culvert did not have the capacity to manage the water volume from the high rainfall therefore storm water runoff through impermeable surfaces was increased at the time.

The final report in Tuve includes collected testimonies regarding observations prior to the landslide. The testimonies indicate that there were issues with surface water during heavy rainfall or snow melt. At the time of the landslide the western area of Tuve Kyrkväg was flooded, but it was not unusual as flooding resulting from damming was frequent [25]. This was partly due to increased less permeable surfaces as a result of urbanization and partly of the low capacity of the culvert to handle all the flowing storm water.

Due to this lacking capacity in handling storm water, The groundwater level in the upper soil layers had recently risen, forcing out foul-smelling pore air [25]. A week before the landslide unusual large water volume accumulated in different places and the amount kept increasing the same day of the landslide.

Additionally to the water problems, minor ground movements with cracks were witnessed in the area [25]. These ground movements are an observation of the fact that the area was under significant strain before the landslide. A crack in the ground measuring 2 to 3 centimeters wide was observed 1 to 2 weeks before the event. The crack was located 120 to 140 meters above the crack that appeared on Tuve Kyrkväg during the landslide.

3.1.4 Reasons behind the failure

A landslide with this extent starts with an initial landslide followed by a secondary landslide. The Tuve landslide is progressive landslide and these typically do not stop until the successive sliding movements reach rock or firmer layers [27].

As mentioned previously, area Tuve Kyrkväg had low stability, and based on the analysis of the movement of the landslide, the initial landslide claims to be triggered there [25]. The steepness of the solid bottom made the slope vulnerable and it had already been strained on the steeper local regions. The high level of precipitation led to a higher groundwater level in the upper soil layers which led to additional strain. Fagerström and Broms show that when the solid bottom slopes, even a slight rise in pore water pressures can trigger landslides, even in cases where the ground surface is almost flat [27].

Derived from Fagerström and Broms demonstration, the increase of pore water pressure and given the already low stability in the area, a successive movement started [27]. Moreover to resist the additional pushing force, forces and the deformations transferred to the end of the slope. These displacements resulted an increase in pore water pressure and decreased soil strength resulting the extensive expand of the landslide.

3.1.5 Conclusion around Tuve

A cooperation of different factors led to the Tuves landslide. There were local areas with low stability along Tuve Kyrkväg which was triggered by the heavy precipitation [25]. Even the urbanization and development in the area increased the strain in the area as well as the water flow through Kville stream resulting ravine erosion. The culverting which was a solution for reinforcement was underdimensioned and unable to handle heavy rainfalls. As a consequence, flooded water in the area was common. The accumulated water would infiltrate the soil increasing pore pressure.

The reason the landslide occurred specifically in 1977 and not before was attributed to the area's development, which introduced incremental changes over time, such as road construction and culverting of the stream[25]. These cumulative alterations gradually contributed to the event .

3.2 Småröd

In 2006, a significant landslide occurred in Småröd north of Uddevalla, bearing similarities to the recent landslide in Stenungsund. Both slope failures profoundly impacted the region during the reconstruction period of Highway E6 and the railway passing through [28]. Prior examinations revealed that the soil in the area primarily consists of clay, with a dry crust overlaying it and a permeable layer beneath, resting on bedrock. This clay was deposited during the glacial period and was determined to have high sensitivity.

The landslide damaged an area of 550 meters by 280 meters were it swept away partly the E6 highway and Bohusbanan railway [**2006AnalysKostnad**]. Besides the infrastructure damage, overhead power lines, properties, and most importantly people were injured. The total cost amounted to 520 million Kronor. The incident led to direct consequences for civilians and industries in the area with the following secondary consequences from closing the damaged and risk area which was a large part of E6.

3.2.1 Reasons behind the landslide

The Swedish Accident Investigation Board released a report regarding the Småröds landslide in 2009. It demonstrates that at the time of the accident the area was exposed to big variations in precipitation according to measurements in the groundwater table [28]. It claims that it is difficult to estimate the effect it had on the landslide. On the other side the new E6 was under construction at the time. The investigation reveals that the northwest part of the area, where a temporary filling was located, passed the limit that it was allowed. This filling was located next to the new E6 highway and investigations determined that this triggered the intial slide. Due to the high sensitivity in quick clay and sloping terrain, the result was a large-scale progressive landslide with piece-by-piece triggered slides.

3.2.2 Conclusion around Småröd

Småröds landslide emphasised the importance of following the limitations given the detailed plan, and how smallest mistakes and changes can lead to devastating consequence both economically and socially. Småröds landslide is an example of human factor being the main trigger behind a natural catastrophe.

3.3 Stenungsund

Stenungsunds landslide is the most recent in Sweden covering an area of 17 hectares, the largest in 46 years [24]. During the night of Saturday, September 23rd, 2023, significant sections of the E6 highway collapsed. The landslide devastated a crucial section of the dual-lane motorway, including its accompanying on and off-ramps, as well as adjacent areas [29].

The restoration of the area is done with the cooperation of Stenungsunds municipality and the Swedish Transport Administration. The Swedish Transport Administration is taking care of restoring the E6 while the municipality is tasked with rebuilding the section of Ucklumsvägen that collapsed and restoring the functionality of Norumsån and its associated network of water, sewage, and district heating pipelines. The restoration is planned to be completed with E6 reopened around early autumn and the turn of the year 2024/2025 [30].

While plans and actions are being implemented to stabilize the area and devise a restoration strategy, investigations into the main cause of the disaster are also in progress. The Swedish Accident Investigation Authority has an ongoing investigation aimed to provide answers regarding the circumstances surrounding the event, including its causes and potential preventive measures for the future. Additionally, the police are investigating the incident to determine if there are any connections to criminal actions leading to the landslide [30].

3.3.1 Reasons behind the landslide

The landslide occurred with the construction of a business park adjacent to the E6 highway in Stenungsund. Different factors are considered in the ongoing investigation. The discovered triggering factors to the day of the report are listed and discussed below.

Lost investigation:

In 2013 the area was investigated to assess the risk of landslide. The stability was measured at multiple locations, where two areas A and C (figure 5) were marked as risk areas. Stenungsunds recent landslide occurred in area C with the greatest risk for instability [31].

Figure 5: Risk areas A and C [31].

Later at the time the whole area converted to Natural land meaning no construction would be allowed in the area [31]. With this change all the associated investigations and data regarding the sensitivity of the ground toward the highway vanished. Furthermore, the municipality approves that the much more resistant A-area sets the standard for the overall load capacity of the entire area meaning that the A-area is described as the worst in terms of stability. However, older documents indicate that the C-area's load-bearing capacity was only half as much load, yet this factor is no longer taken into account.

Later the areas type changes and the construction of the new business park is approved. The lost data about the sensitivity of the land sloping towards the E6, result in wrong basis for detail planning the project [31]. An approval was granted for a substantial elevation of the ground level through increasing the volume of embankment material from approximately 4000 to 16000 cubic meters, without conducting a risk assessment for landslides in the area. Nonetheless, the municipality ultimately approves filling the embankment with approximately six meters of soil, where the land has collapsed.

Inaccurate investigations:

The soil and geotechnical investigations of the construction of the business park were conducted by the company Norconsult on behalf of Badhustorget Private Residences AB [32].

Investigations in the area exhibit five different soil conditions: sand, clay, glacial river sediment, till, and bedrock [33].

The area consists of organic soil with a layer of sand/loamy sand with a thickness of approximately 1–4 m [34]. This is followed by a clay layer with a thickness of about 3–5 meters with quick properties. The clay rests on a layer of friction soil lying on bedrock. The friction soil has a thickness of approximately 0.5–1.5 m. The depth to solid bedrock was measured throughout the subarea to be between approximately 4 and 9 m.

After analyzing the data, a map detailing the geotechnical and hydrogeological conditions of the area was created and included in the Technical Project Report [34]. Additionally, the stability of the area has been assessed in various sections. According to calculations for both present and future scenarios, the current safety against landslides meets the established standards, provided that the ground is not subjected to a load exceeding 50 kPa. Loads directly placed on bedrock are not subject to load restrictions. However, if larger loads are anticipated anywhere else than bedrock, further examinations is necessary.

If all the calculations indicated stability, why did the landslide occur? Subsequent investigations following the landslide revealed inaccuracies in the presented geotechnical map of the area [35]. The part that collapses was supposed to consist of bedrock (see figure 6) but today this shows that the presentation provided in the investigation is inaccurate.

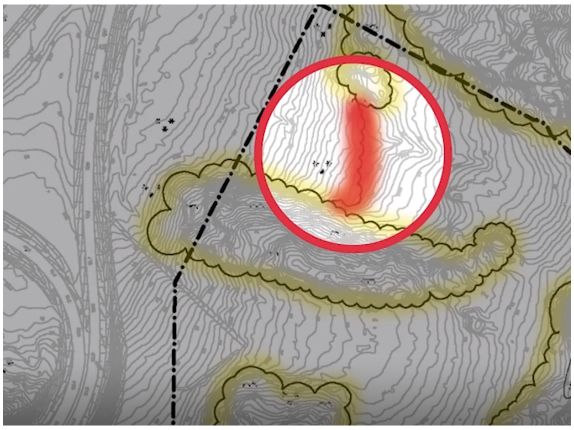

Figure 6: The red area marked in the figure was presented to consist of bedrock close to surface but it did not [35]

According to the Swedish Geotechnical Institute, the inaccurate map influenced their assessment of landslide risk before construction [35]. If the bedrock had not been marked on the slope, the agency would likely have recommended further investigations and stability calculations.

Reckless endangerment:

According to the latest investigations and newly discovered evidence, three individuals are suspected of gross public dangerous negligence, gross causing bodily harm and unauthorized environmental activities [36]. The suspects had connections to a company that was constructing on the hill where the assumed initial landslide occurred.

Prosecutor Daniel Pettersson reveals that a large volume of excavation material was dumped on the upper part of the slope without permission nor appropriate measures being taken [37]. According to the prosecutor this external excavation of 74000 cubic meters, corresponds to a load three times bigger than what was allowed.

With all above being said the current suspicion is that human influence is behind the landslide where soil was triggered by an excessive load more than what was allowed on the ground.

3.3.2 Conclusions around Stenungsund

In conclusion, there is no evidence to prove a natural cause behind the Stenungsunds landslide. However a various human influence in different forms is evident. This includes lost documentation and incomplete preliminary studies before the construction as well as incompetent and reckless decisions within the construction area. It is worth to mention that the factors discussed above are the existing and under investigation possibilities to the day of this report and nothing is proved and presented to the general as a finished investigation-report.

3.4 Gjerdrum, Norge

On Wednesday, December 30, 2020, just before 4:00 am, a quick clay landslide with a volume of 1,35 million cubic meters occurred in the municipality of Gjerdrum. Eleven people as well as an unborn child lost their lives and over 1600 were evacuated [38].

After the landslide, the government of Norway gathered a public expert committee in February 2021 to investigate the event [39]. The goal was to firstly investigate the causes behind the landslide and secondly provide its assessments and recommendations for future management of quick clay and landslide risks in Norway.

The investigation into the causes of the landslide has taken various factors into account and thoroughly analyzed them. It has examined whether different construction projects or measures in the area may have influenced the occurrence of the event [39]. Additionally, physical evidence, witness observations, as well as geotechnical and hydrological investigations and calculations are used to determine the process and type of the landslide.

3.4.1 Landslides placement

The landslides origin is confirmed to be in the slope between Holmen farm and the Tistil stream south of Ask center [39]. The stability of the slope was calculated to be very poor with large parts of quick clay. studying the terrain models and satellite pictures over the years indicated significant erosion in the Tistil stream. During the period from 2007 to 2015, the base of the slope experienced vertical erosion of a total of 2.5 meters. Additionally, the streambed gradually shifted sideways towards the east, along the slope.

3.4.2 Erosion

While erosion is a natural phenomenon, Tistil stream erosion was unusually intense [39]. The hydrological investigations indicate that the erosion has been amplified by change in the land use and urbanization. Urbanization leads to more dense surfaces and reduced vegetation. This results to faster runoffs.

In connection to agricultural planning in the 1980s, efforts were made to manage watercourses more effectively. This included placing sections of the Tistil Stream into pipes [39]. Over time Tistil Stream subsequently broke out of the pipes, likely starting towards the end of the 1990s. This breakout resulted in the streambed shifting mainly eastward from its original position. The displacement caused increased erosion of the slope's base at Holmen as the stream dug into the surface. These changes, including both lateral movement and vertical erosion, led to the decreased stability of the slope.

3.4.3 Environmental factors

There are meteorological and hydrological data indicating high precipitation from December 26th to 29th, 2020, right before the occurrence of the landslide [39]. The weather was unusually mild which prevented frost, this made it possible for maximal infiltration leading to increased soil saturation. Different model simulations indicate that the soil saturation level ranged between 90 and 100 percent right before the occurrence of the landslide.

The steady flow of water over a long period increases the pore pressure in the quick clay, pushing clay minerals to go apart [39]. The weakened strength from the high pore pressure along with the high water flow in the stream, which may have caused additional erosion just before the landslide, made the overall stability of the slope at its worst.

3.4.4 Conclusion around the Gjerdrum

The Gjerdrum landslide shares many similarities with the Tuve incident. Elevated pore pressure due to heavy rainfall, urbanization, and its impact on water runoff are all contributing factors to both landslides.

In conclusion as the reason behind the event, the committee claims the main triggering factor to be the large amount of infiltrated water in the soil before the landslide which resulted in one or more small slips along the eastern side of the Tistil Stream, in the slope below Holmen. The several slips initiated retrogressive landslide development where each sliding portion leaves behind a new unstable slope/edge. The large extent of the landslide which had a Span of approximately 2 Km indicated the presence of a large amount of quick clay in the area.

While heavy precipitation occurred in 2000 as well, no landslide occurred at that time. The reason is explained by the erosion of the stream at the slope over time.

The breakout of the stream from the pipes may have resulted in more turbulent flow and increased erosion.

In conclusion, heavy precipitation and Various forms of human activities by urbanization and pipe installation have contributed to increased erosion in the Tistil Stream leading to reduced stability of the slope and the margin against landslides. The committee believes that if the Tistil stream was prevented and protected from erosion in time, the landslide would likely not accrue.

4 Climate change and its impact on slope stability

This segment will explore the phenomenon of global warming and its anticipated impact on the likelihood of landslides. Data from the scenario models created by the Intergovernmental Panel on Climate Change (IPCC) will be applied in theory to investigate how the expected climate change will affect the parameters of quick clay.

4.1 Global water cycle

The water cycle is affected by diverse factors both climatic and non climatic. The cycle is the naturally occurring movement of water and mass transformation. One of the most crucial factors to consider is the consequences of a warmer temperature in terms of changes in the water cycle. A warmer climate means that the air can store more moisture. This in addition to the increase in evaporation entails a most likely intensification in precipitation and soil moisture [40]. IPCC suggests that the influence of the anthropogenic period has affected the water cycle significantly compared to preindustrial conditions. The greatest storage of water is contained in glaciers alongside in the oceans. The resolution of glaciers and intensified evaporation due to temperature changes is a probability to consider when discussing slope stability.

4.2 Scenario and pathway modeling

In the sixth assessment report [41], IPCC presents a new method for predicting climate scenarios in the future. The work is specifically focusing on five different scenarios with each one divided in near term (2021-2040), mid term (2041-2060) and long term (2061-2100). The variation between the models is based on assumptions regarding the shared socio-economic pathway and the predicted global effective radiative forcing in 2100.

Alterations in the atmosphere and land use pose a high risk related to the earth's energy budget, that is the total net energy entering or leaving the system, contributing to warming or cooling effect [42]. This includes anthropogenic actions such as the emission of greenhouse gases, and aerosols, deforestation, and excavation of natural resources. To quantify these changes IPPC outputs an effective radiative forcing, Wm^{-2} which indicates how the climate system reacts to these perturbations, in terms of feedback in physical, biogeophysical, and biogeomechanical processes. Predictions point to accumulation in the energy budget at least until the 21st century despite considering extensive mitigation scenarios.

4.3 Landslides

Warming of the earth undoubtedly affects the stability of natural and engineered slopes and has consequences in terms of landslides [3]. Water has a big influence on the stability of the soil. Some of the problems related to changes in the hydrology may be a lower amount of rain required to reach the critical level for a slope to fail. These critical conditions occur when the flow and discharge increase eroding the banks as well as the resulting groundwater table changing both the effective stresses and the shear strength of the material. Besides this, an increased seepage is likely to enhance the gravitational forces and can be explained as the resultant body force of the slope [15]. The weight of the wet soil will also increase which means greater gravitational forces triggering the slides. Some of the constructed engineering slopes may have to be reevaluated since the increase in precipitation poses high demands on the drainage [3]. If the capacity of the system is insufficient, water may be redirected to unfavorable directions which can have devastating consequences on the stability and erosion of supporting areas.

Artesian pressure occurs when groundwater is confined within an aquifer or geological formation under pressure. This pressure is typically caused by the low permeability and weight of overlying rock or soil layers, which restrict the flow of water [43]. In the case of artesian pressure, the increased pressure within the confined aquifer can act as an uplift force enhancing the risk of landslides. Besides this, it can reduce the effective weight and frictional resistance of soil or rock layers on a slope. This reduction in friction can make the slope more susceptible to failure and movement. Increased precipitation will most likely enhance the problems related to artesian pressure in underlying soil layers.

Side effects of global warming could very well benefit the stability as well. Higher temperature resulting in greater volumes of water being evaporated from the surface contributes to a decrease of groundwater table and water content, hence a large amount of water is needed to reach critical conditions of slip surfaces. However, the extent of the future water cycle and how the soil will behave is very difficult to estimate, but according to the scenario models the infiltration and precipitation are most likely to be greater than the expected evaporation [5]. Quick clay is typically found in Sweden and Norway with a latitude of approximately 60 degrees. Figure 7 shows the projected result in precipitation subtracted by the evaporation one can conclude that there is a positive resulting value that can infiltrate or runoff from surfaces.

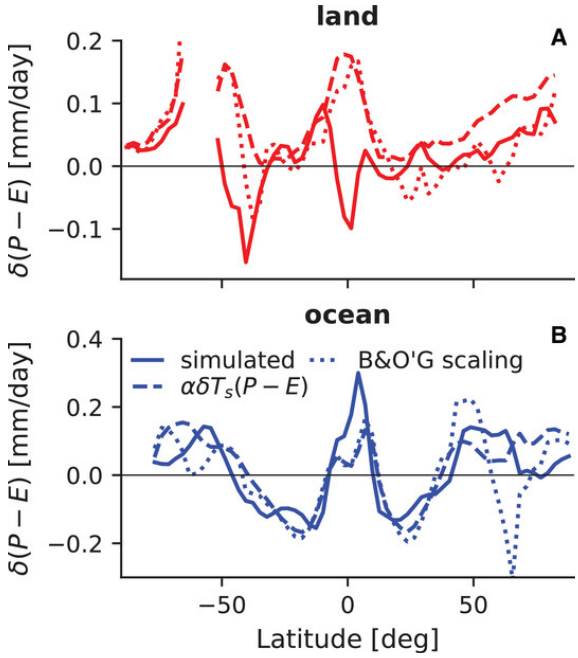

Figure 7: Projected change in water cycle at certain location. [40]

Vegetation stands out as a reliable factor capable of mitigating landslide occurences. It is considered a cost-effective and sustainable approach to minimize geohazards in soil [44]. Despite its recognized influence on slope stability, uncertanties remain regarding the magnitude of its inpact. Plant roots play a crucial role in stabilizing soil by penetrating it, thereby enhancing shear strenght. However, estimating the effect of vegetation on drainage capacity remains challenging. Nevertheless, vegetation facilitates water removal from the soil, thus increasing the particle strenght while reducing material weight. In a rapidly changing climate, vegetation holds a promise as a significant element in counteracting fluctuating water content and increased water tables.

4.4 Influence on parameters

The IPCC's 2018 report on global warming [5], indicates that the frequency of extreme weather occurrences such as intense rainfall and heatwaves is bound to rise worldwide. As a result, there will likely be an increase in water levels, changing soil conditions and increasing the risk of landslides. The effective stress is influenced by both initial stress levels and pore water pressure. Higher water levels result in reduced effective stresses, as noted by [45], [15], leading to a weakening of soil strength. In Equation (1), shear strength is determined by the effective cohesion and stress, which is influenced by the internal friction angle of the soil. Therefore, it can be inferred that a reduction in effective stress will entail a weakening of the soil strength.

$$\tau = c + \sigma * tan(\phi) \tag{1}$$

Furthermore, a reduction in suction stresses is anticipated as a result of loss of negative pore water pressure. On top of that wet soil also tends to be denser, resulting in increased gravitational forces that impact stability [46]. The impact can vary across different regions primarily due to variations in soil permeability and the time required for the water to infiltrate.

In their study, Kafle et al. investigated slope stability influenced by fluctuations in precipitation and reservoir levels in China [46]. They monitored precipitation patterns and reservoir elevations to calculate corresponding safety factor values. Their analysis revealed that the safety factor was heavily influenced by changes in water elevation rather than precipitation intensity. A decrease in reservoir levels immediately correlated with a reduction in the safety factor. Even after the water level returned to its initial level, there was a delay in the restoration of the safety factor which can be seen in figure 8 . However, there is likely to be a connection between precipitation intensity and water elevation even though there is a delay due to infiltration time.

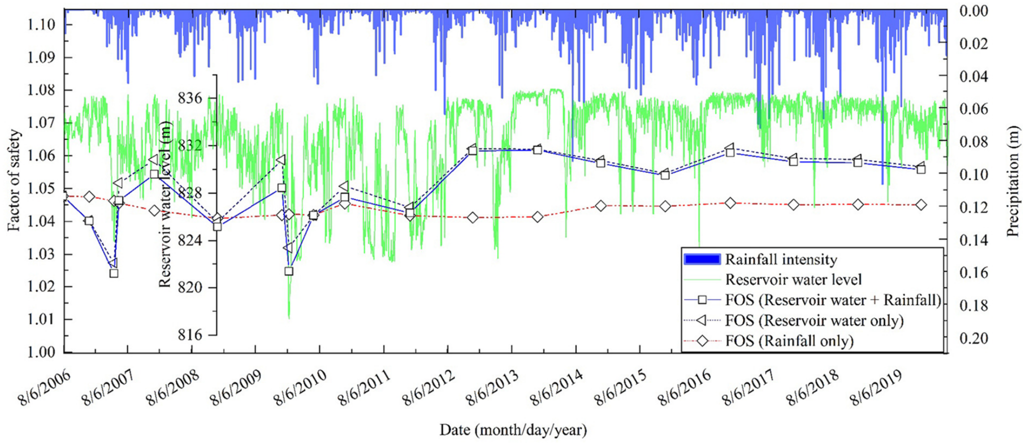

Figure 8: Factor of safety dependant on fluctuation in precipitation and water elevation. [46]

Unsaturated soil, often referred to as the capillary zone, is characterized by being partially saturated with negative pore water pressure. While the general principles associated with shear strength in saturated soil can be applied to unsaturated soil, there are additional factors to consider. As demonstrated in Equation 1, soil strength depends on the Mohr-Coulomb failure criterion, which incorporates effective stress and friction angles. However, in unsaturated conditions, another factor must be taken into account, capillary suction [47]. Equation 2 introduces the second term controlled by matric suction and phi´, a soil parameter defining the relationship between shear strength and soil suction. The suction effect is manifested by the difference between pore air pressure and pore water pressure. As the water pressure approaches the air pressure, the soil's behavior begins to resemble that of saturated soil, as described by Equation 1.

$$\tau = c + \sigma * tan(\phi) + (ua - uw) * tan(\phi) \tag{2}$$

In practical scenarios, the portion of total shear strength influenced by matric suction is frequently overlooked due to uncertainties in estimating its effect [47]. Factors such as precipitation and fluctuations in weather conditions can lead to wetting of layers with negative pore water pressure, eliminating the suction stresses and consequently decreasing the shear strength.

5 Simulations in Geostudio

The chosen section to analyze is the case of Tuve. For the simulations, a sequence of the layers in the soil has been estimated with a dry crust in the first two meters followed by a thick layer of clay which has been divided into two categories as seen in Figure 9. This is mainly based on the cone penetration tests performed in the area which indicate an increase in Shear strength in the first layer followed by a decrease in the second one [6]. This graph is shown in the appendix A. On top of the bedrock, a frictional layer with high conductivity is expected to generate high artesian pressure triggering the failure.

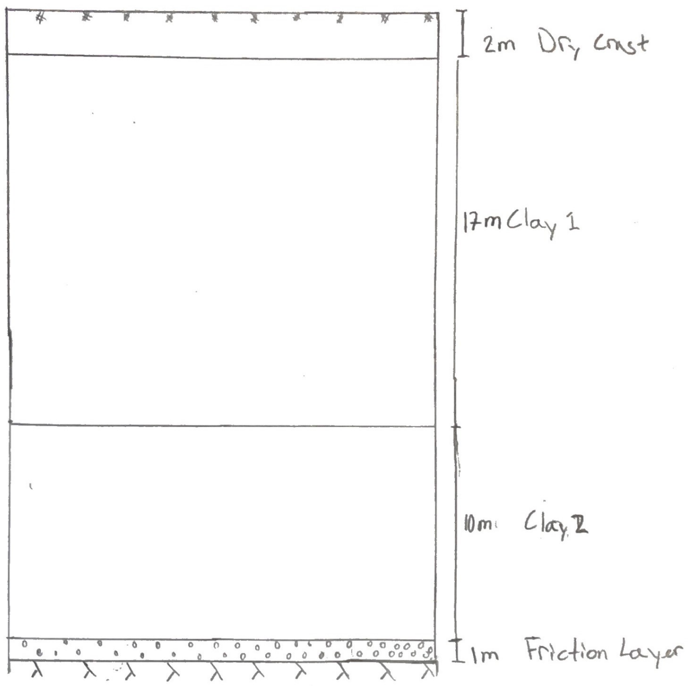

Figure 9: General Cross section and soil layer of the Tuve Area illustrated by authors.

Figure 10 shows the sequence observed in Tuve by eyewitnesses. The goal of the simulations was to show which section was the crucial one with the potential to trigger the progressive landslide. A crack in area one is thought to be one of the reasons for the failure. Hence for better understanding, a shallow slide in section B was analyzed.

Figure 10: Serial behavior in Tuve slide. [25]

5.1 Combined analysis

The unique soft clay in Scandinavia has resulted in an approach to shear strength in a combined matter. The factor of safety is a calculation of both undrained and drained analysis in which the lowest result is used to get a conservative safety factor. The maximum value used in Geostudio is the undrained (C_u) which can be seen in figure 11.

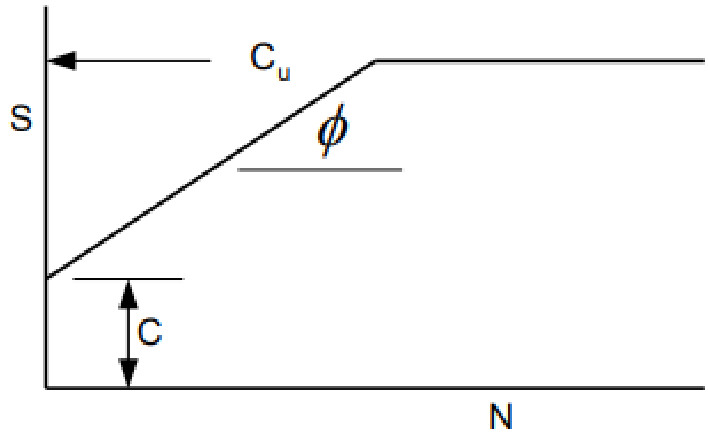

Figure 11: Combined shear strength analysis with different methods. [48]

5.2 Factor of safety

Slope stability calculations are based on the limit equilibrium method which uses two different equations. One equation provides the safety factor with respect to moment equilibrium (3) and the other gives the safety factor with respect to forces equilibrium (4). The principle is to divide the body into several pieces with calculations for each one and consequently summed into a final factor of safety. Figure 12 shows the forces acting on one of the sections described.

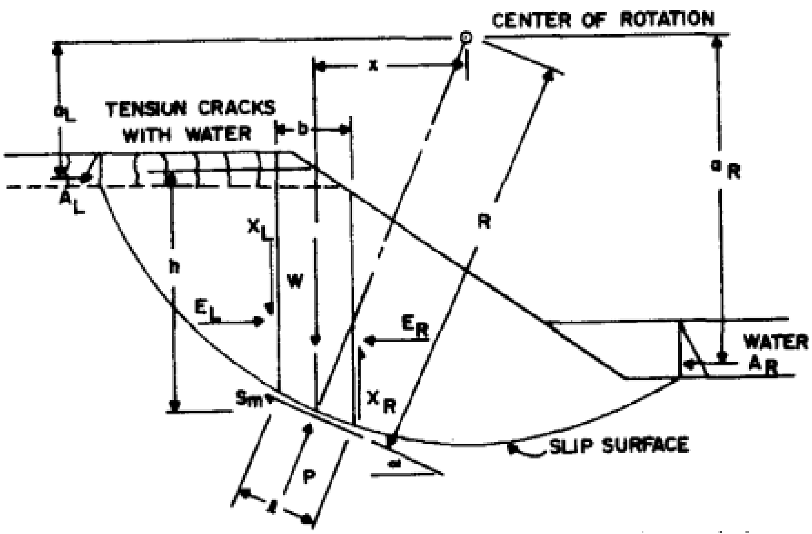

Figure 12: Acting forces in a circular slip surface [49]

Below are the equations shown with corresponding parameters.

$$Fm = \frac{\sum(c + (N - \mu\beta)R\tan\phi)}{\sum Wx - \sum Nf - \sum Dd} \tag{3}$$

$$Ff = \frac{\sum(c\beta\cos\alpha + (N - \mu\beta)\tan\phi\cos\alpha)}{\sum N\sin\alpha - \sum D\cos\omega} \tag{4}$$

$$\begin{aligned}
\text{where:}\quad c &= \text{effective cohesion} \\
\phi &= \text{effective angle of friction} \\
u &= \text{pore-water pressure} \\
N &= \text{slice base normal force} \\
W &= \text{slice weight} \\
D &= \text{concentrated load} \\
\beta, R, x, f, d, \omega &= \text{geometric parameters} \\
\alpha &= \text{inclination of slice base}
\end{aligned}$$

The key parameter in both equations N, the normal force at the base of the slope is obtained by summing the vertical forces of each slice. The slice base normal is dependant on the interslice shear force on each side of the slice.

$$N = \frac{W + (XL - XR) - \frac{c\beta\sin\alpha + u\beta\sin\alpha\tan\phi}{F}}{\cos\alpha + \frac{\sin\alpha\tan\phi}{F}} \tag{5}$$

Among the several available versions of the limit equilibrium method LEM, the interslice shear force, X handled in the equations is based on an equation proposed by Morgenstern and Price [50].

$$X = E\lambda f(x) \tag{6}$$

$$\begin{aligned}
\text{where:}\quad f(x) &= \text{a function} \\
\lambda &= \text{the percentage of the function used} \\
E &= \text{the interslice normal force} \\
X &= \text{the interslice shear force}
\end{aligned}$$

The factor of safety in Morgenstern-Price method is calculated to satisfy both the moment equilibrium and force equilibrium. By changing λ in the interslice shear function a value of the safety factor which satisfies both the force equilibrium and moment equilibrium is obtained (see figure 13).

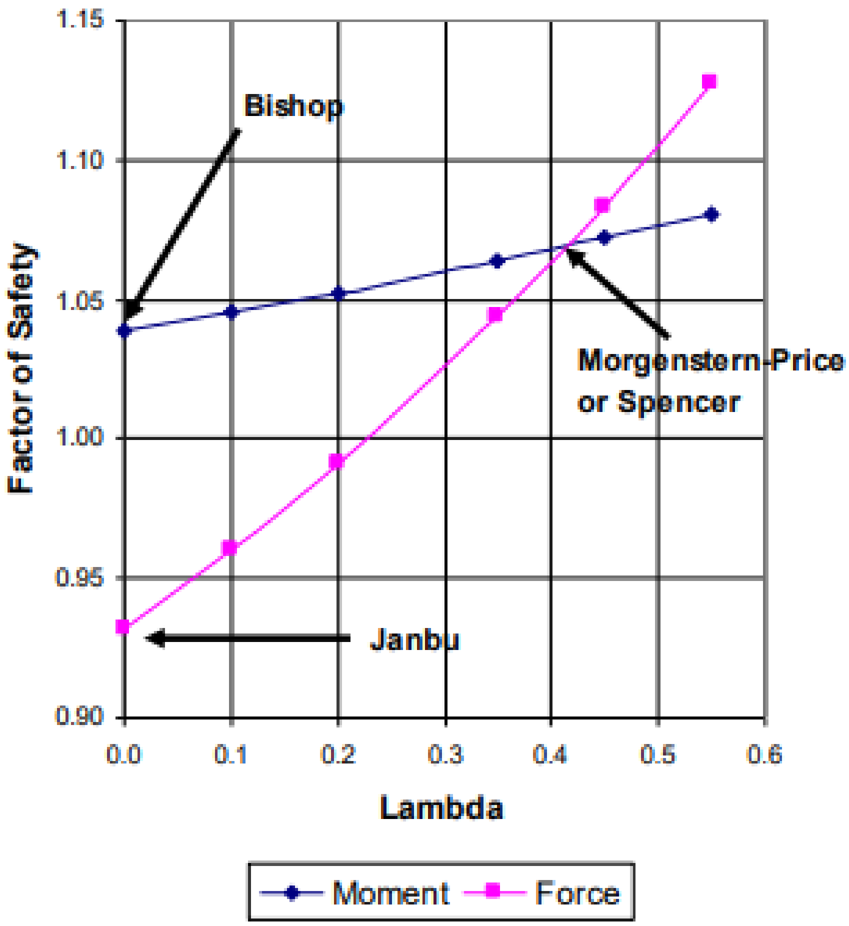

Figure 13: Iteration process to obtain factor of safety [48]

5.3 Calculation stages

The analysis is based on three different analyses. The first one which is the parent analysis is controlled by a initial state of groundwater table. The table is constructed manually at a water head located two meters below the ground surface based on literature data. The next step is to apply infiltration show in table 1, a flux Q equal to 120 millimeters over the duration of 30 days at the surface representing the heavy rain in November 1977 before the slide. There was dry period compared with regular amount in the month before the slide and assumptions have been made that cracks are present in the analysis. They are estimated to reach the total dry crust of two meters depth being filled with water.

Name	Category	Kind	Parameters
Infiltration	Hydraulic	Water flux	5e-08 m/sec

Table 1: Applied infiltration as a boundary condition in seep/W

6 Results

This chapter will present the results from both the literature part of the study and the Geostudio simulations. Whether the simulations represent the real case of Tuve will be discussed and compared to Trafikverkets requirements.

6.1 Results from literature

The geology of an area one can provide valuable insights into the potential presence of quick clay. Understanding this helps us map out areas of risk and additional safety measurements can be implemented when planning for construction. With an understanding of the composition and properties of the quick clay, we can trace back what causes these landslides at a particle level. The historical landslides highlight the importance of the human factor. While the natural factor is also significant, the anticipated increase in precipitation can be attributed to climate change, which is traced back to human activities.

There are similarities in the cases that we have analyzed. In all areas, there is likely to be quick clay present, and they all have a geological formation that poses an increased risk of landslides. Human factors as in urbanization and ongoing construction projects have either affected the stability negatively or contributed to erosion as in the cases of Tuve and Gjerdrum. The weather conditions in Tuve and Gjerdrum are also an important factor that reduces the soil stability, making the areas more vulnerable. Although the case of Stenungsund is not fully evaluated, similarities to the previous cases can be observed, both with the geological aspect and ongoing construction.

6.2 Results from monitoring in inSAR

Looking at satellite images from inSAR unusually large settlements are observed where the landslide later occurred. In figure 14 one can see a clear correlation between the red dots and the area later involved in the landslide. The data is from 2015-2021 and the settlement over time is displayed in figure 15.

Figure 14: Area in Stenungsund where the landslide occurred. Dots represent a value in which the movement of the ground in the y axis has changed over time. [51]

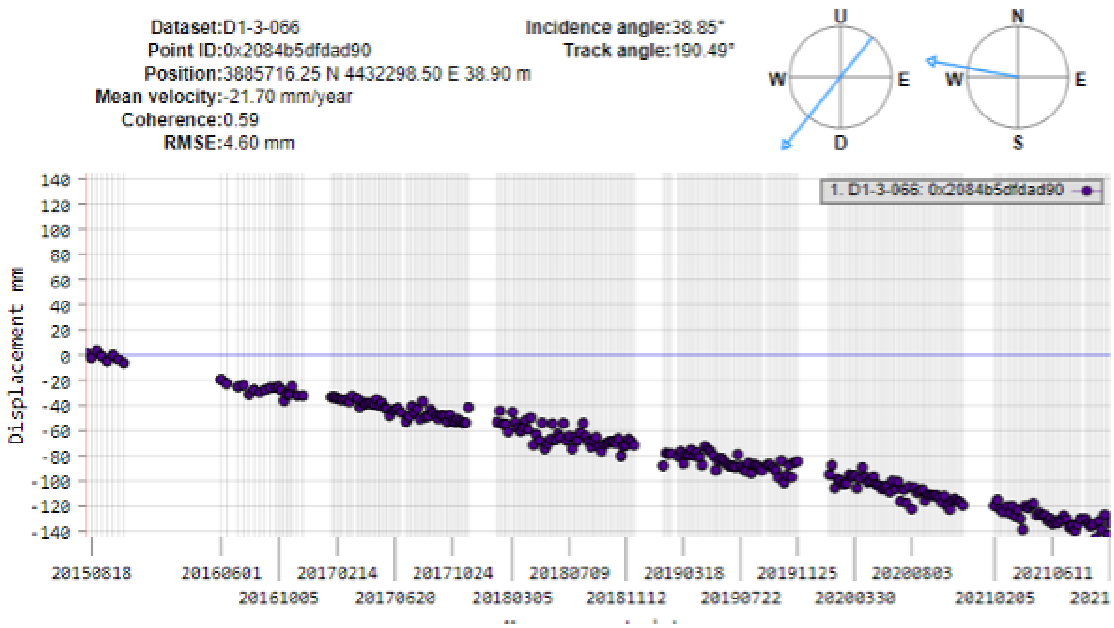

Figure 15: Movement of chosen point from 2015 to 2021 in millimeter. [51]

6.3 Results from Geostudio

Trafikverket classifies quick clay in the third category meaning one should use characteristic values for all loads and material parameters when dimensioning a construction [52]. The third safety class is applied concerning stability failure for construction on quick clay and the values are presented in table 2.

Safety classification	Undrained analysis	Combined or drained analysis
1	1.35	1.2
2	1.5	1.3
3	1.65	1.4

Table 2: Requirements from Trafikverket regarding safety factors for different scenarios

The safety factor against slope failure for the most probable slip surface in the soil during construction shall be at least the value specified for the third safety factor. The lowest acceptable value for the safety factor is 1.65 for undrained analysis and 1.4 for combined or drained analysis. Table 3 compiles our results.

Section	Safety factor
A-A	1.624
B-B	0.904
B-B	2.529
C-C	1.305

Table 3: Safety factors from Simulations in Geosudio

The results provided by our simulations fail to meet the Technical Requirements in sections B (for the shallow slip surface) and C.

The following figures show our results from the simulations.

6.3.1 Section A-A

Color	Name	Model	Unit Weight (kN/m³)	Cohesion' (kPa)	Phi' (°)	C-Top of Layer (kPa)	C-Rate of Change ((kN/m²)/m)	Cu-Top of Layer (kPa)	Cu-Rate of Change ((kN/m²)/m)
	Berg	Bedrock (Impenetrable)							
	Friktionslager	Mohr-Coulomb	17	0	30				
	Lera1	Combined, S=f(depth)	16		30	1.5	0.15	20	0.5
	Lera2	Combined, S=f(depth)	16		30	1.5	0.15	30	-0.5
	Torrskorpa	Mohr-Coulomb	15	0	30				

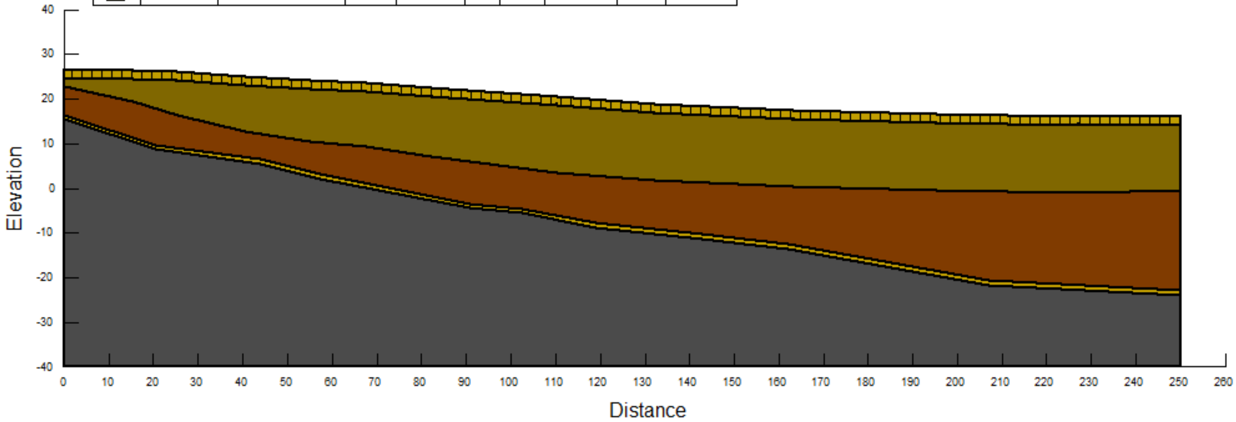

Figure 16: Soil layers in section A-A.

Figure 16 presents the sequence of soil layers for section A-A with their properties respectively.

Cobr	Name	Model	Vol. WC. Function	K-Function	SatKx (m/sec)
	Berg	Saturated Only			1e-20
	Friktionslager	Saturated / Unsaturated	Friktionslager	Friktionslager	
	Lera1	Saturated / Unsaturated	Lera1 WC	Lera HC	
	Lera2	Saturated / Unsaturated	Lera2 WC	Lera HC	
	Torrskorpa	Saturated / Unsaturated	Torrskorpa WC	Torrskorpa HC	

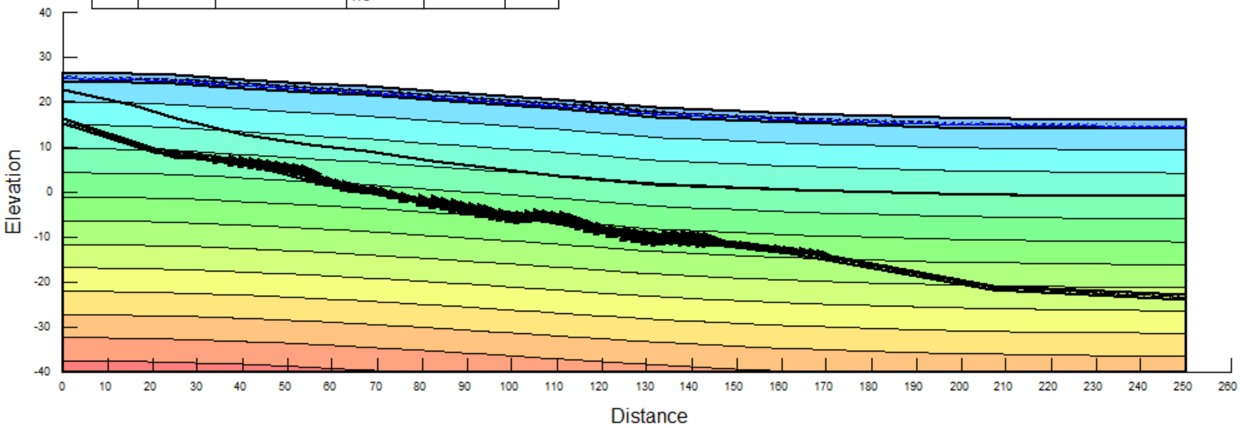

Figure 17: Initial conditions in section A-A.

Figure 17 shows the initial water flow in section A-A by arrows in the friction layer where the size of the arrows is proportional to the flow. Initial conditions mean the flow before infiltration starts.

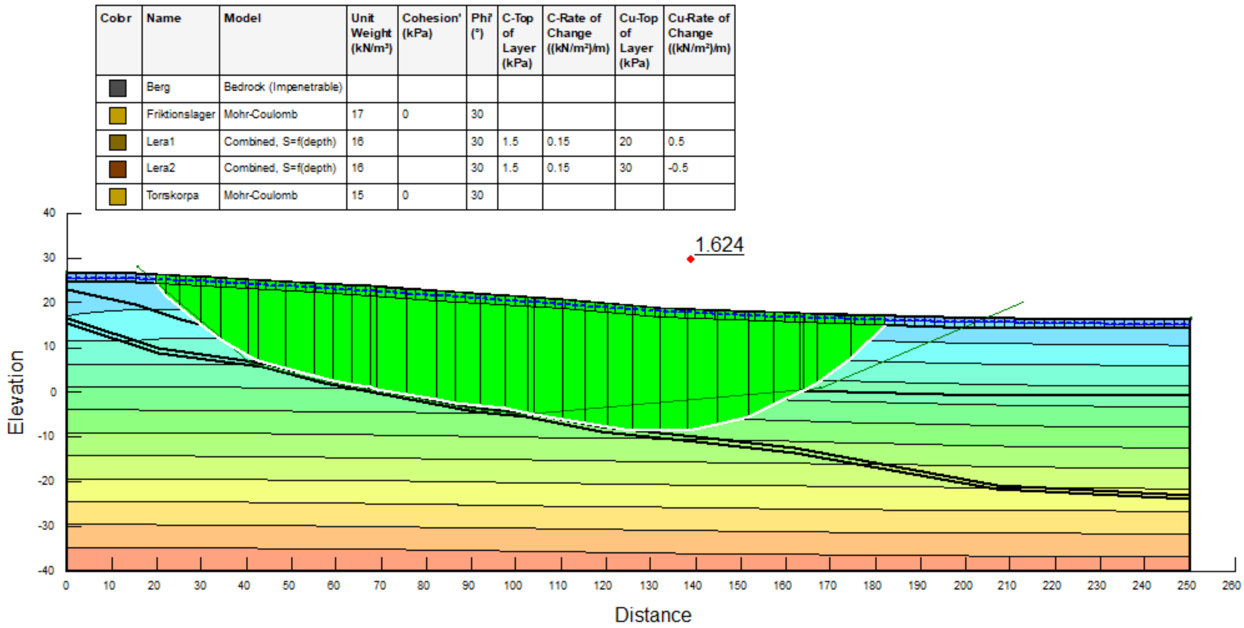

Color	Name	Model	Unit Weight (kN/m³)	Cohesion' (kPa)	Phi' (°)	C-Top of Layer (kPa)	C-Rate of Change ((kN/m²)/m)	Cu-Top of Layer (kPa)	Cu-Rate of Change ((kN/m²)/m)
	Berg	Bedrock (Impenetrable)							
	Friktionslager	Mohr-Coulomb	17	0	30				
	Lera1	Combined, S=f(depth)	16		30	1.5	0.15	20	0.5
	Lera2	Combined, S=f(depth)	16		30	1.5	0.15	30	-0.5
	Torrskorpa	Mohr-Coulomb	15	0	30				

Figure 18: Factor of safety at time = 0 in section A-A.

Figure 18 shows the calculated safety factor equal to 1.624 at the initial phase without infiltration.

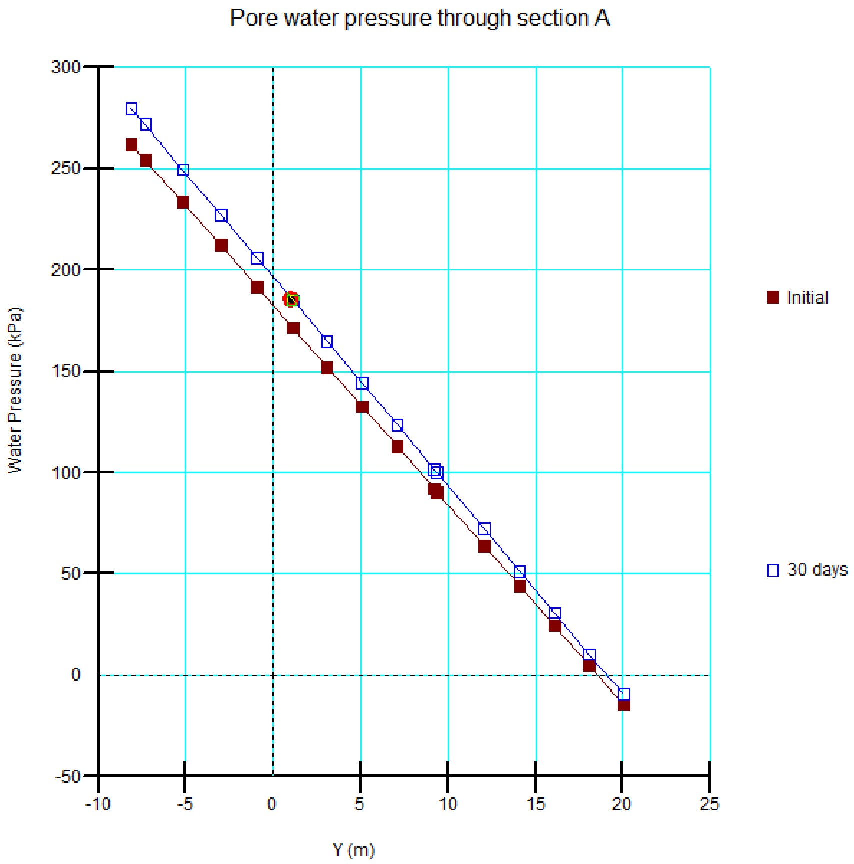

Figure 19: Pore water pressure through section A-A at the start and after 30 days. The conditions viewed are located at a distance of 116 meters.

Figure 19 shows the pore water pressure trend line changing from the initial case without infiltration, to an increased trend line after 30 days of infiltration.

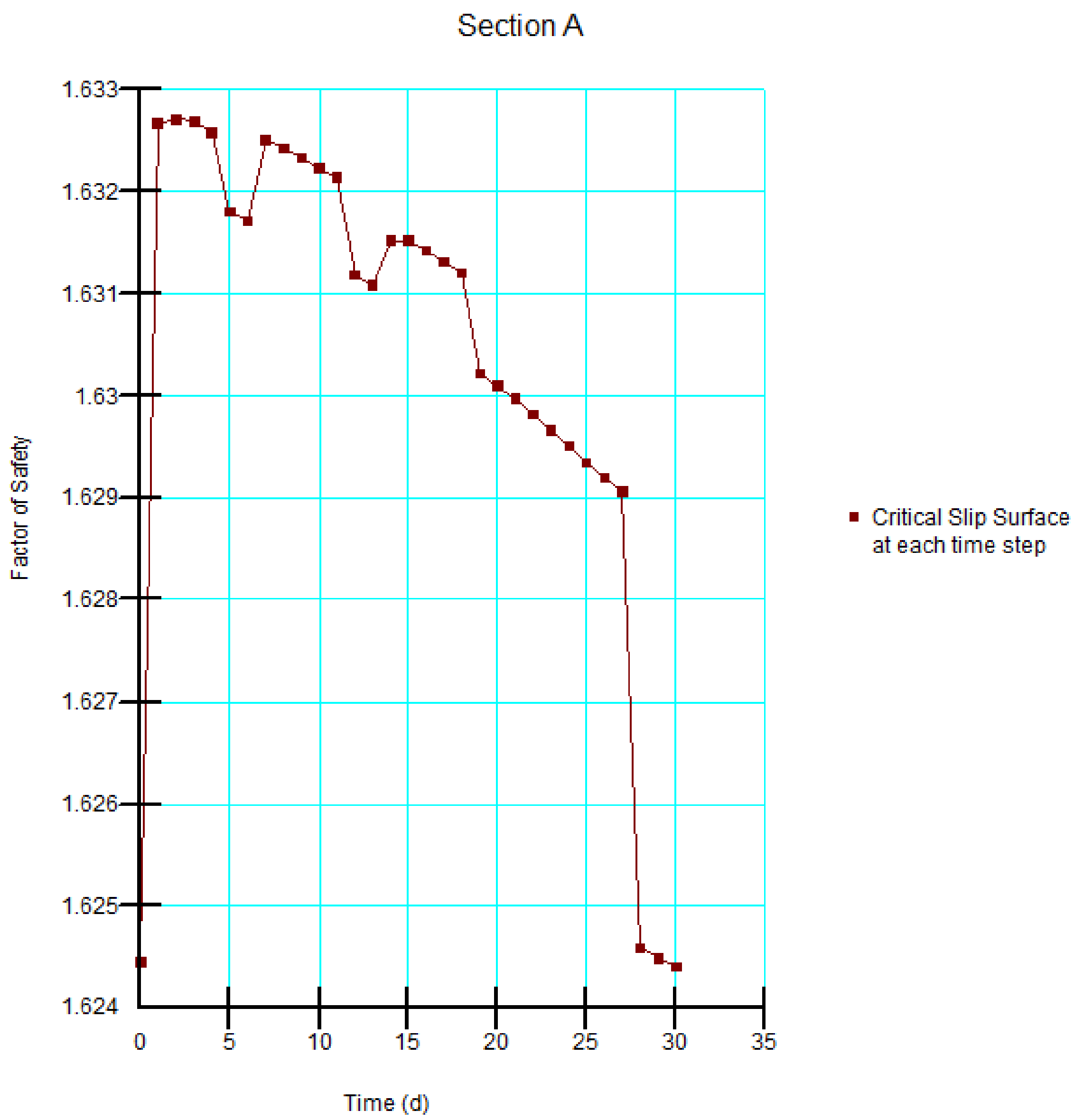

Figure 20: Change of safety factor in section A-A.

Figure 20 shows the change in safety factor over the slip surface in section A-A over a period of 30 days.

6.3.2 Section B-B

Color	Name	Model	Unit Weight (kN/m³)	Cohesion' (kPa)	Phi' (°)	C-Top of Layer (kPa)	C-Rate of Change ((kN/m²)/m)	Cu-Top of Layer (kPa)	Cu-Rate of Change ((kN/m²)/m)
	Berg	Bedrock (Impenetrable)							
	Friktionslager	Mohr-Coulomb	17	0	30				
	Lera1	Combined, S=f(depth)	16		30	1.5	0.15	20	0.5
	Lera2	Combined, S=f(depth)	16		30	1.5	0.15	30	-0.5
	Torrskorpa	Mohr-Coulomb	15	0	30				

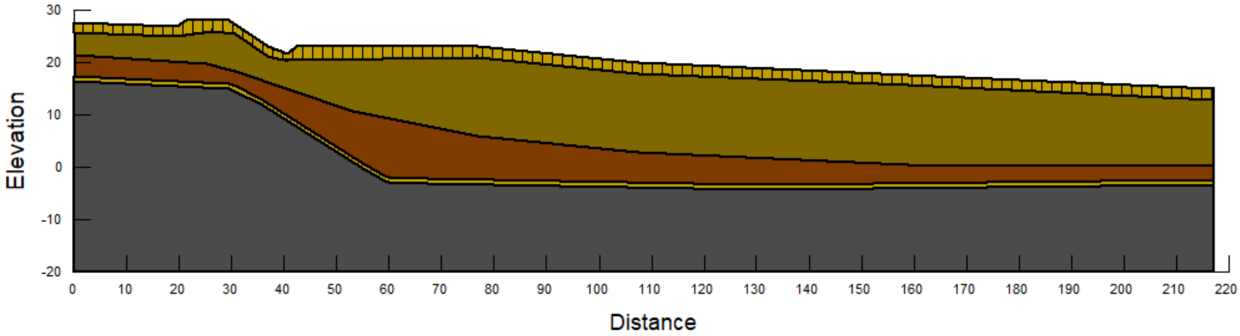

Figure 21: Soil layers in section B-B.

Figure 21 presents the sequence of soil layers for section B-B with their properties respectively.

			Function	
	Berg	Saturated / Unsaturated	berg	Berg HC
	Friktionslager	Saturated / Unsaturated	Friktionslager	Friktionslager
	Lera1	Saturated / Unsaturated	Lera1 WC	Lera HC
	Lera2	Saturated / Unsaturated	Lera2 WC	Lera HC
	Torrskorpa	Saturated / Unsaturated	Torrskorpa WC	Torrskorpa HC

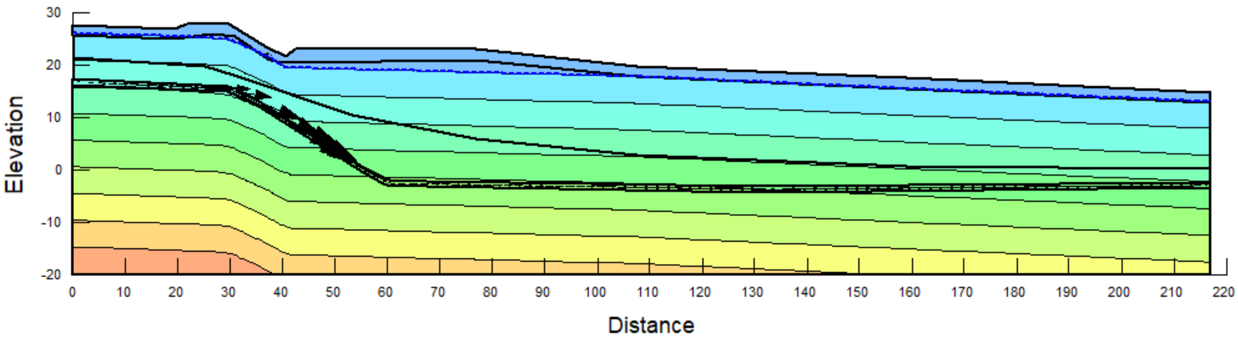

Figure 22: Initial conditions in section B-B.

Figure 22 shows the initial water flow in the friction layer for section B-B before infiltration.

Color	Name	Model	Unit Weight (kN/m³)	Cohesion' (kPa)	Phi' (°)	C-Top of Layer (kPa)	C-Rate of Change ((kN/m²)/m)	Cu-Top of Layer (kPa)	Cu-Rate of Change ((kN/m²)/m)
	Berg	Bedrock (Impenetrable)							
	Friktionslager	Mohr-Coulomb	17	0	30				
	Lera1	Combined, S=f(depth)	16		30	1.5	0.15	20	0.5
	Lera2	Combined, S=f(depth)	16		30	1.5	0.15	30	-0.5
	Torrskorpa	Mohr-Coulomb	15	0	30				

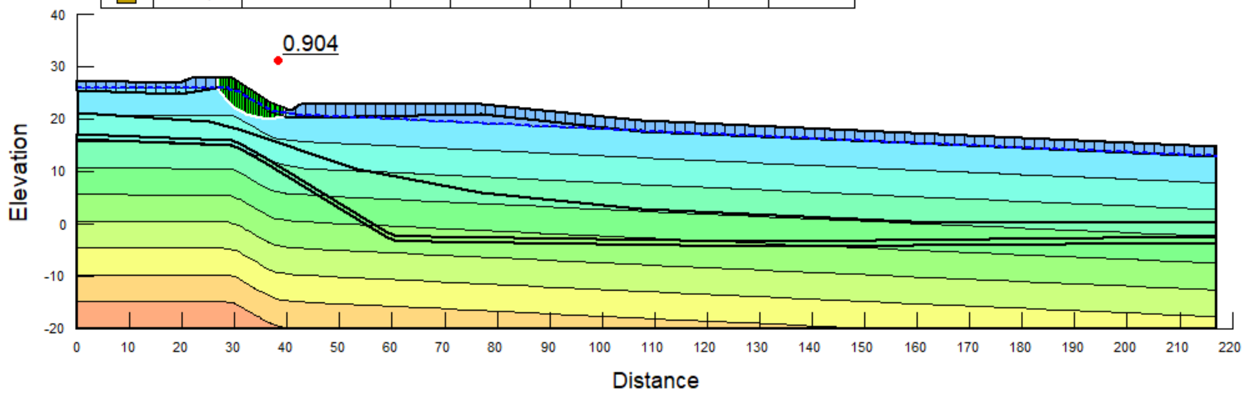

Figure 23: Safety factor of the marked slip surface in time=0 for section B-B.

Figure 23 shows the initial safety factor for the local slope marked in the figure calculated as 0.904. The safety factor being below 1 indicates failure in slope.

Color	Name	Model	Unit Weight (kN/m³)	Cohesion' (kPa)	Phi' (°)	C-Top of Layer (kPa)	C-Rate of Change ((kN/m²)/m)	Cu-Top of Layer (kPa)	Cu-Rate of Change ((kN/m²)/m)
	Berg	Bedrock (Impenetrable)							
	Friktionslager	Mohr-Coulomb	17	0	30				
	Lera1	Combined, S=f(depth)	16		30	1.5	0.15	20	0.5
	Lera2	Combined, S=f(depth)	16		30	1.5	0.15	30	-0.5
	Torrskorpa	Mohr-Coulomb	15	0	30				

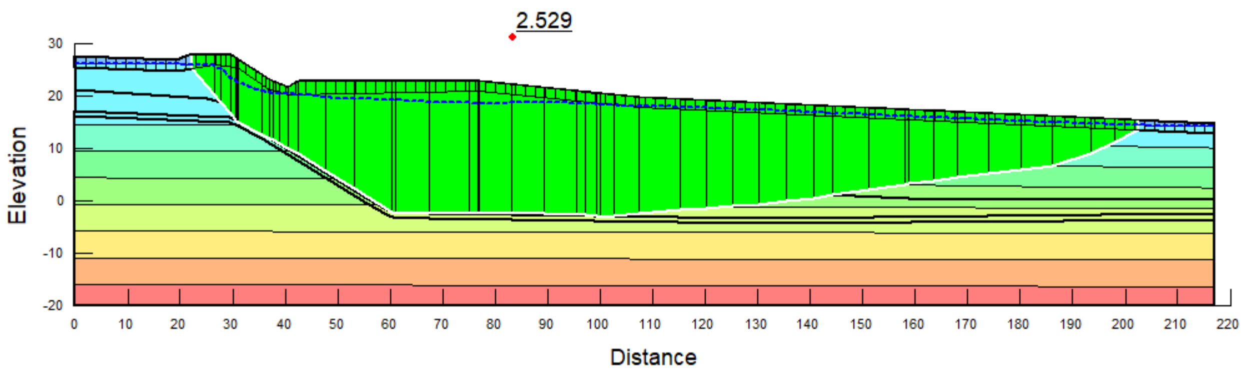

Figure 24: Factor of safety for a bigger slip surface at time = 0 in section B-B.

Figure 24 shows the calculated safety factor to be 2.364 of the slope with a larger covering slip surface.

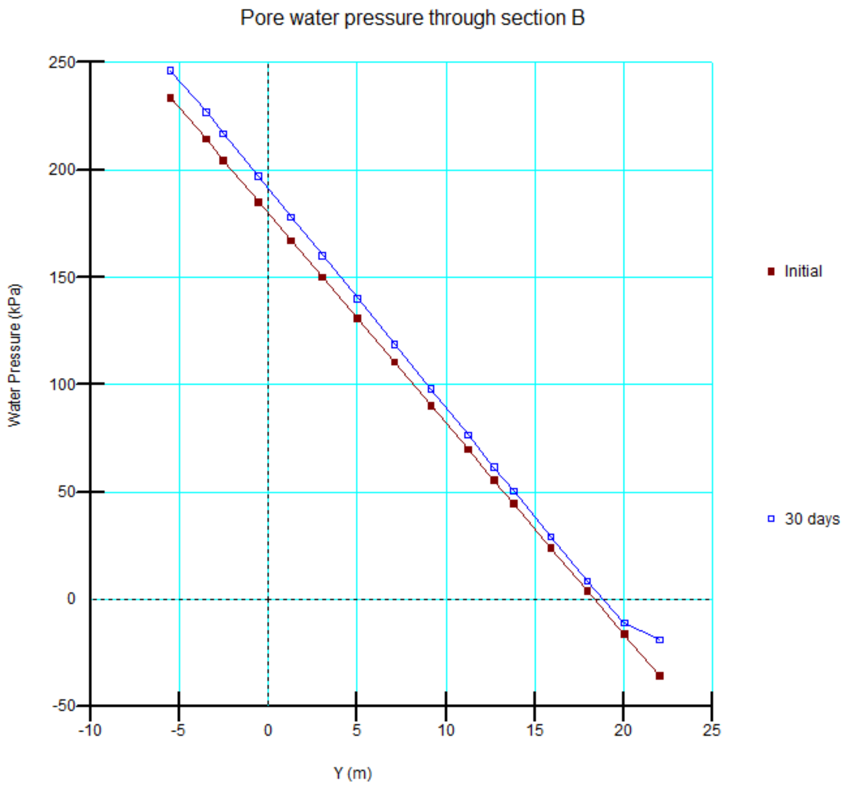

Figure 25: Pore water pressure through section B-B at the start and after 30 days. The conditions viewed are located at a distance of 85 meters.

Figure 25 Shows the pore water pressure trend line increasing after applying infiltration for 30 days.

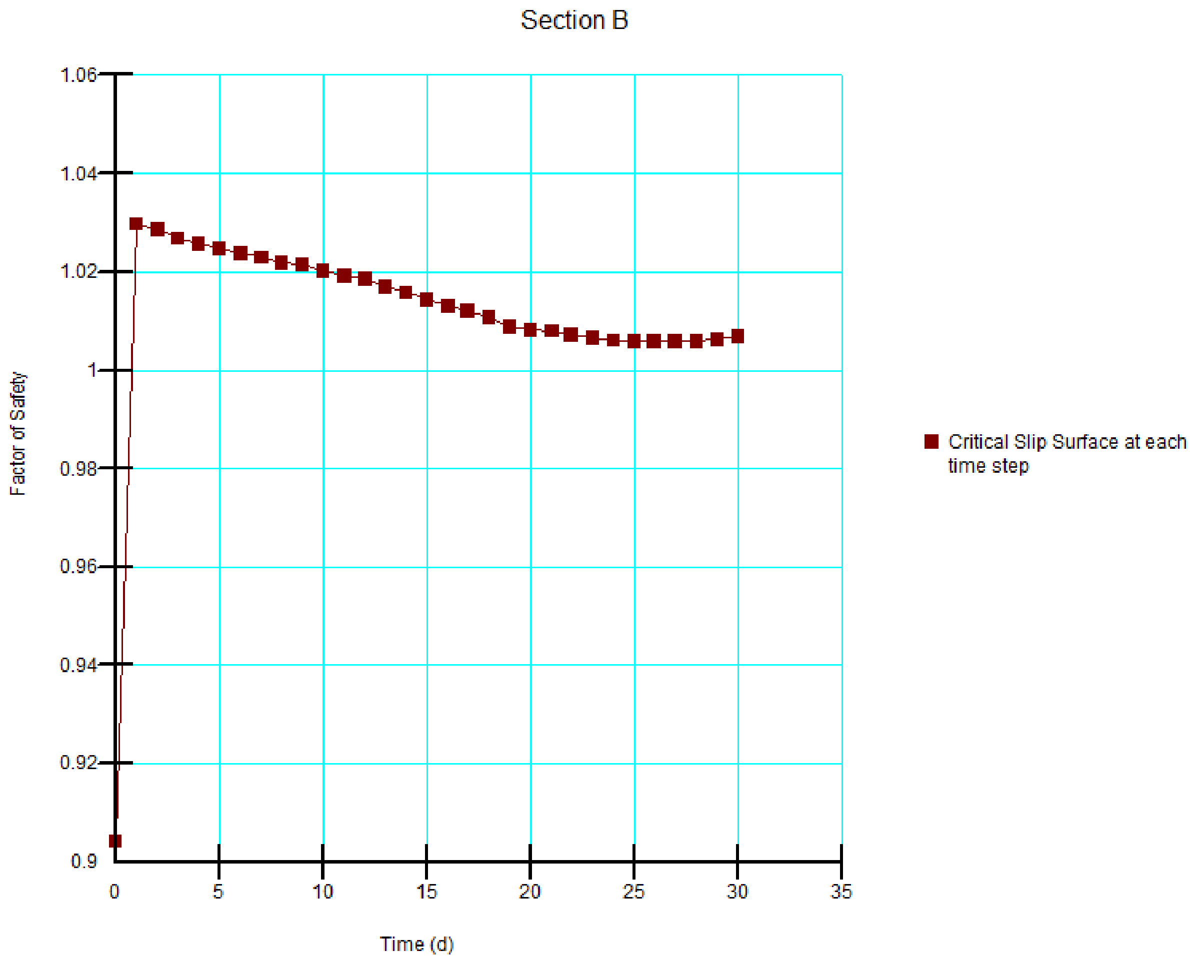

Figure 26: Factor of safety for the local/smaller slip surface in section B-B.

Figure 26 shows the change in the factor of safety for the local slip surface at section B-B.

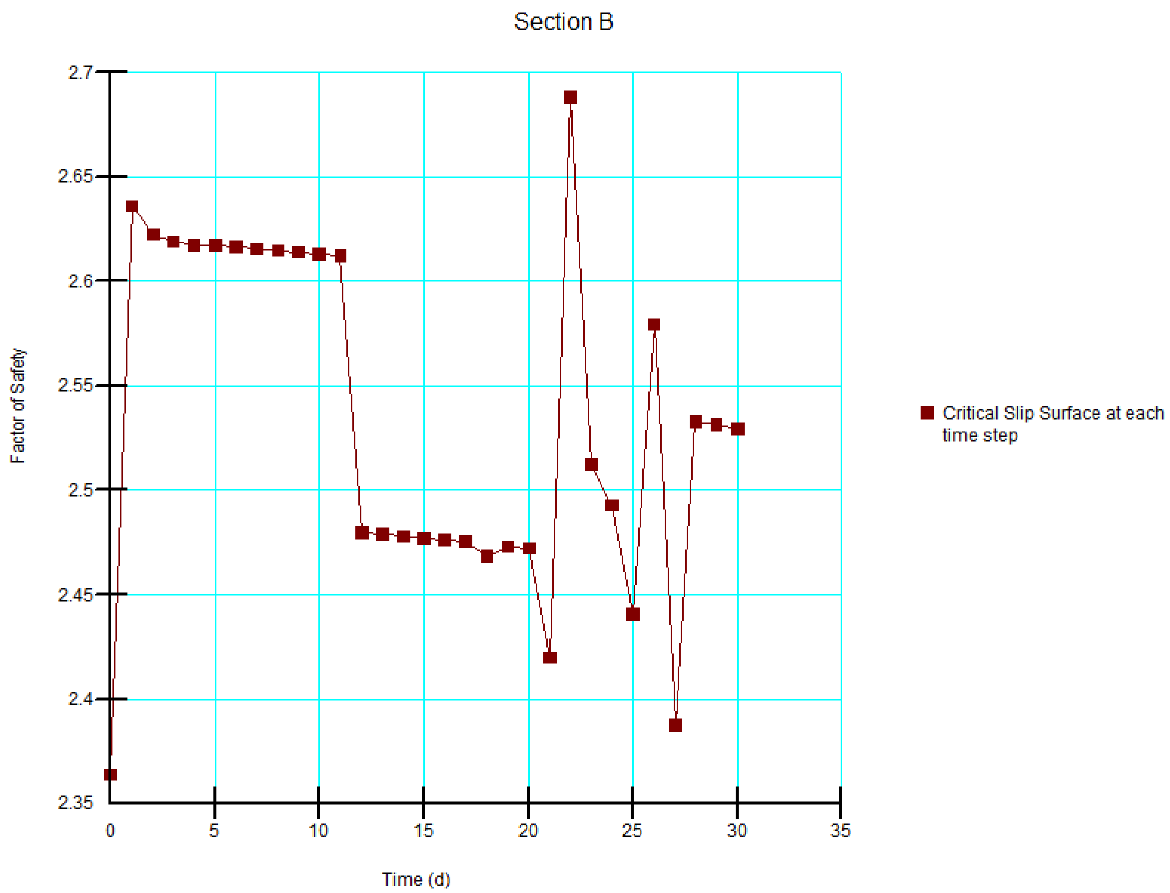

Figure 27: Initial conditions in section B-B.

Figure 27 shows the change in the factor of safety in the larger slip surface in section B-B.

6.3.3 Section C-C

Color	Name	Model	Unit Weight (kN/m³)	Cohesion' (kPa)	Phi' (°)	C-Top of Layer (kPa)	C-Rate of Change ((kN/m²)/m)	Cu-Top of Layer (kPa)	Cu-Rate of Change ((kN/m²)/m)
	Berg	Bedrock (Impenetrable)							
	friktionslager	Mohr-Coulomb	17	0	30				
	Lera 1	Combined, S=f(depth)	16		30	1.5	0.15	20	0.5
	Lera2	Combined, S=f(depth)	16		30	1.5	0.15	30	-0.5
	Torrskorpa	Mohr-Coulomb	15	0	30				

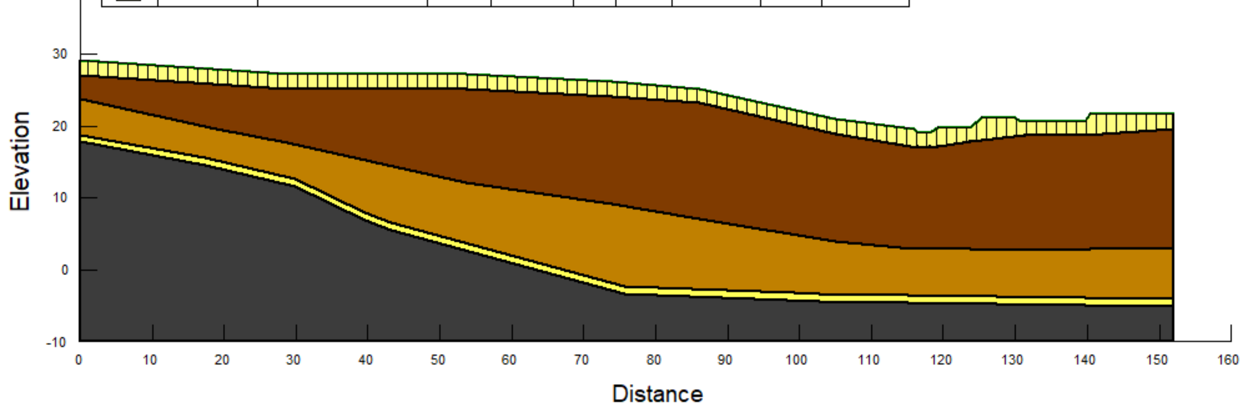

Figure 28: Soil layers in section C-C.

Figure 28 presents the sequence of soil layers for section C-C with their properties respectively.

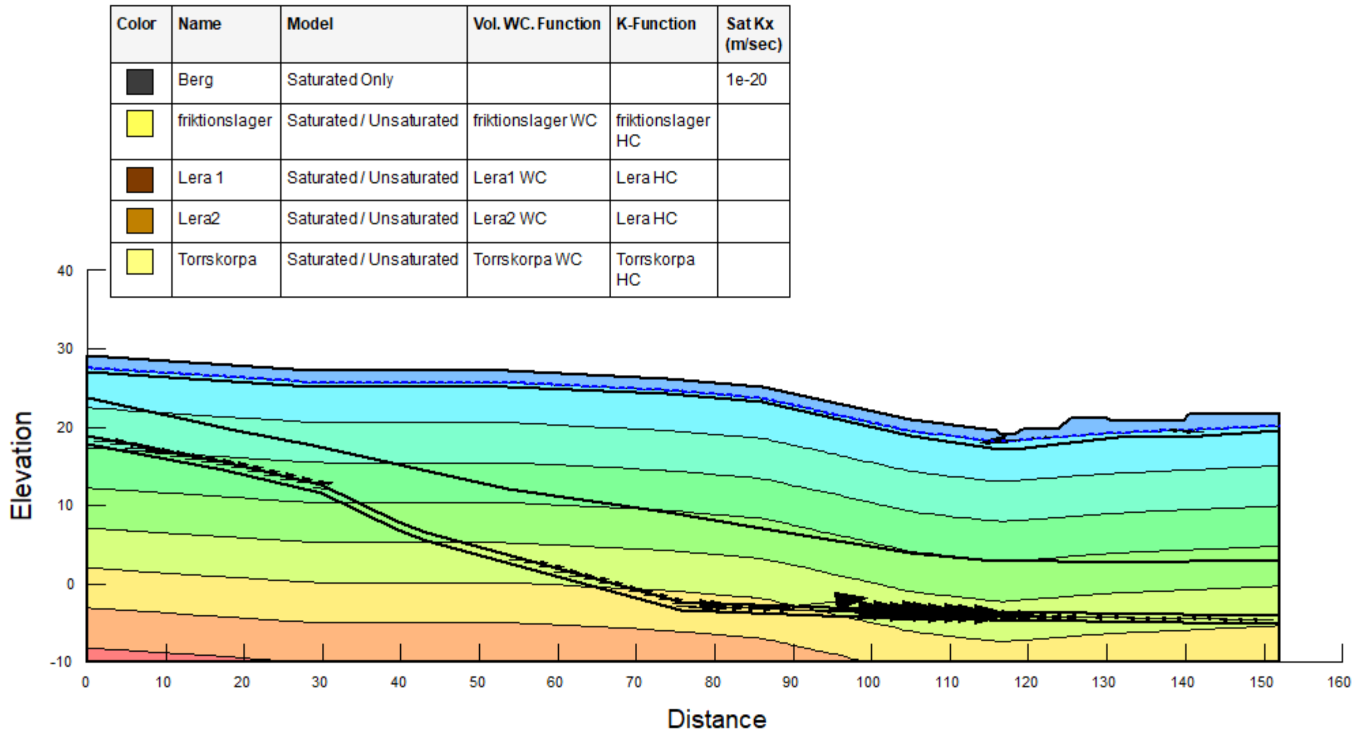

Figure 29: Initial conditions in section C-C

Figure 29 Shows the water flow in the friction layer of section C-C before infiltration.

Color	Name	Model	Unit Weight (kN/m³)	Cohesion' (kPa)	Phi' (°)	C-Top of Layer (kPa)	C-Rate of Change ((kN/m²)/m)	Cu-Top of Layer (kPa)	Cu-Rate of Change ((kN/m²)/m)
	Berg	Bedrock (Impenetrable)							
	friktionslager	Mohr-Coulomb	17	0	30				
	Lera 1	Combined, S=f(depth)	16		30	1.5	0.15	20	0.5
	Lera2	Combined, S=f(depth)	16		30	1.5	0.15	30	-0.5
	Torrskorpa	Mohr-Coulomb	15	0	30				

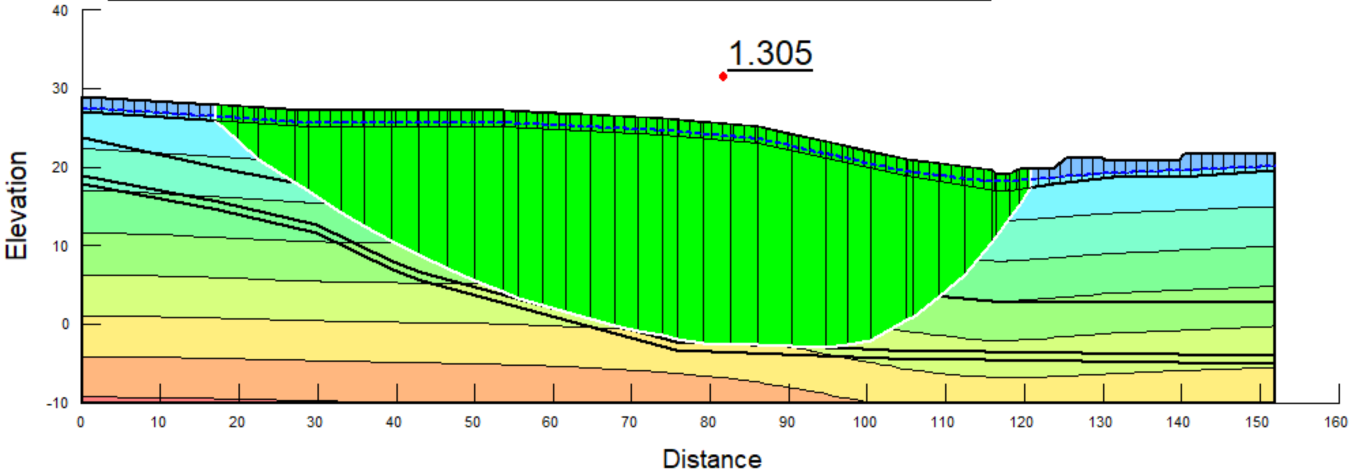

Figure 30: Factor of safety at time = 0 in section C-C

Figure 30 shows the calculated safety factor equal to 1.305 in section C-C before infiltration starts.

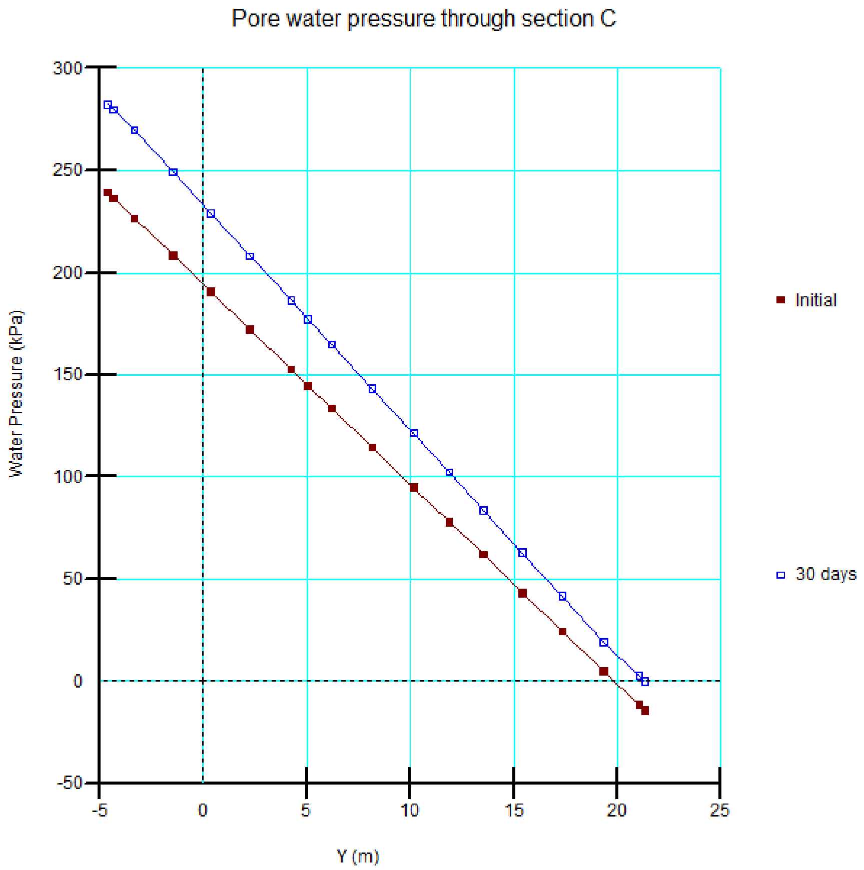

Figure 31: Pore water pressure through section C-C at the start and after 30 days. Conditions viewed are located at a distance of 103 meters.

Figure 31 shows the increase in pore water pressure trend line from the initial phase and after 30 days of infiltration.

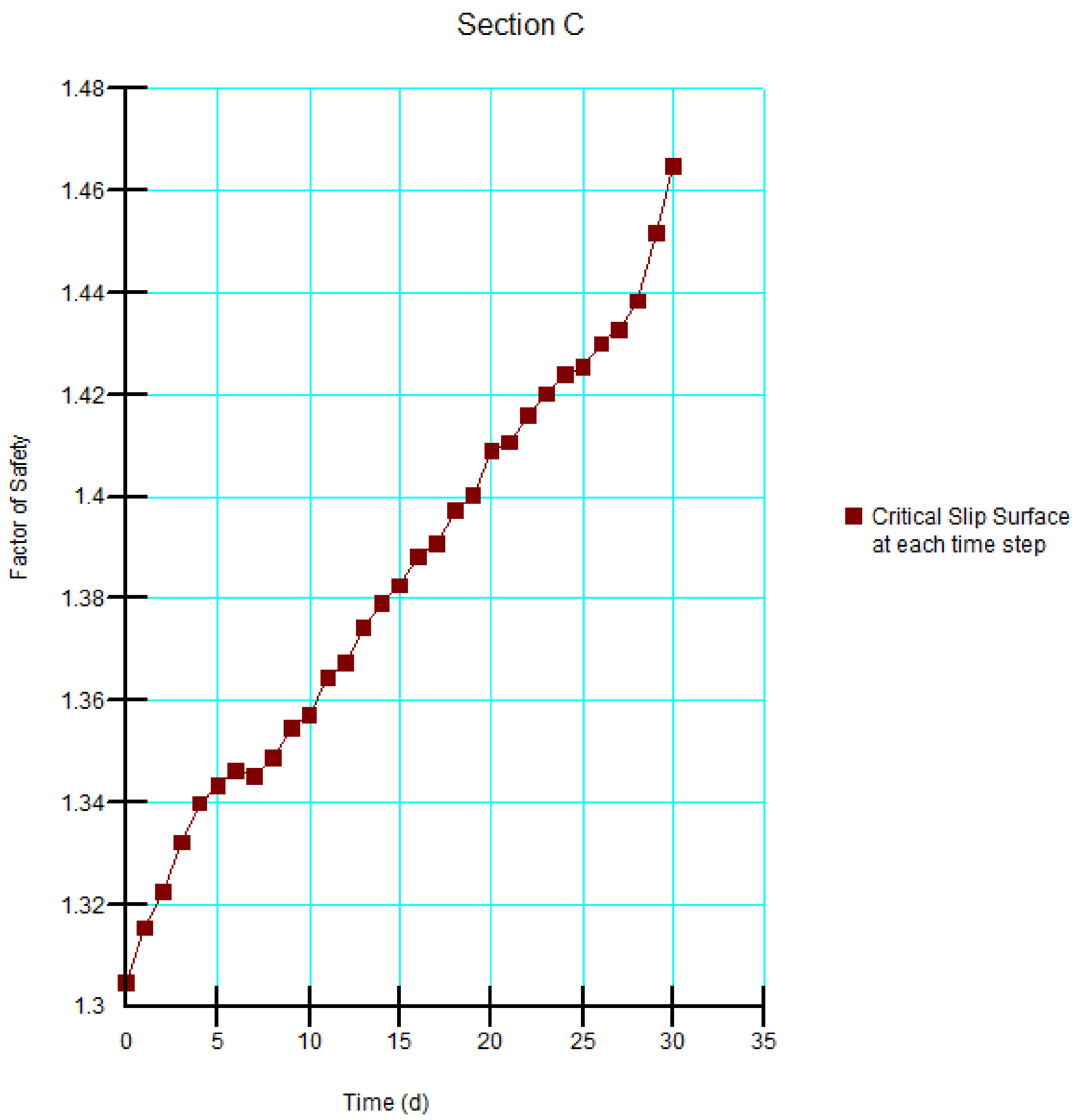

Figure 32: Initial conditions in section C-C.

Figure 32 shows the change in safety factor during the infiltration period from day 0 to day 30.

7 Conclusion and summary of simulations

One aspect this report covered was to investigate whether and how climate change will impact the stability of quick clay. The literature review reveals that the primary processes affecting the stability due to climate change are heavy precipitation with the following consequences. This includes changes in the ground water table altering the shear strength of the soil, changing water pressure, and increasing flow which can create erosion and high artesian pressure in frictional layers consequently leaching salt from adjacent clay.

In the real case of Tuve, it was believed that the failure began in zone 1 according to figure 10. The direction of this slide was from the crack at Tuve kyrkväg towards Nya kyrkvägen. This indicates that the sections influenced in this area are primarily B and C. Our simulations also support this. In section B two different sliding surfaces were investigated. The shallow slide initiated from the crack in figure 23 is concluded to trigger the initial landslide in the chosen slip surface with an initial safety factor of 0.904. This failure was initiated by water, creating conditions for a serial behavior in the form of progressive behavior. This is shown in figure 10. The initial shallow landslide in section B resulted in bigger slides in other sections that followed due to ground movements and loss of support at the bottom of the slope.

This is verified in the model where the obtained safety factor with initial conditions in the larger sections is 1.624 in A, 2.529 in B, and 1.305 in C. All of these sections are considered stable but once a disturbance is present in quick clay an unpredictable behavior is expected with figure 10 visualizing this sequence. In figure 32 the factor of safety is visualized over a period of 30 days with the changes in the transient analysis. The factor increases from 1.305 to 1.465. This change is difficult to interpret because according to conclusions from theory and literature, it should decrease. This result is generated due to the water accumulating downwards in the section. This elevation contributes to a higher value since it is located in the lower passive zone of the slide. Another factor that could mitigate the result is the lack of build-up pore water pressure in the frictional layer. The frictional layer does not reach the surface in the analysis which results in limited flow in that section.

The sliding body in the sections is seen as a translational progressive landslide since it is a gently inclined slope with a local failure that progresses along the slip surface creating a body. Step two in the serial behavior of progressive slides deals with disturbances and in this case, a perturbation is the pore water changes and built-up water pressure in the frictional layer. In figure 31 the change in pore water pressure can be seen and be estimated to be approximately 50 kPa. A change in this value will have a significant decrease in the shear strength of the soil. This initial slide was the beginning of a slide that influenced greater areas. The movement in the ground and loss of support might trigger other sections to fail. The safety factor is very high in sections A and B but, as a consequence of the first slide, a subsequent behavior expands to other parts.

The simulations reveal significant flow within both the frictional layer and the dry crust. In the month leading up to the Tuve landslide, 120 millimeters of rain was recorded in the area. Before this, there was a period of drought compared to typical conditions. This suggests that the dry crust experienced capillary suction, resulting in negative pore water pressure that strengthened this layer. However, with increased water levels, flow, and the absence of cracks, this pressure is reduced, altering the shear capacity of the crust. Using flow vectors, it is observed that the frictional layer tends to facilitate water passage beneath the thick clay. This creates a vulnerable zone which is the weakest link. Several factors contribute to this vulnerability, including diffusion through nearby clay and the leaching of salt, which weakens the layer at the bottom. This zone is where an initial slide is anticipated to occur. Furthermore, the loss of frictional support and erosion will further decrease the safety factor of the slope.

The climate analysis indicates that different scenarios affect water pressure. Furthermore, the analysis suggests that each parameter is affected by climate change. Regarding the connection between water pressure and groundwater, it is estimated that pressure will increase depending on the geographic location and season in Sweden. Climate change is associated with an increase in the frequency and intensity of extreme weather events, such as storms, hurricanes, and heavy rainfall. These events can trigger landslides and slope failures by rapidly saturating the soil and increasing surface runoff, leading to erosion and instability.

7.1 Uncertainties and assessment of results

One source of error is related to the insufficient amount of geotechnical data available from the Tuve area. In this study, it has been assumed that pore pressure could form in the friction layer. However, no data is confirming whether the friction layer reached the surface anywhere in the area or if it only was present in certain parts. If the friction layer never reaches the surface, flow generated in the layer is restricted by the mighty layers of clay, resulting in less significant pore pressure buildup in the models. This can be seen in figure 25 where a pore water distribution is presented through the section. There is a hydrostatic behavior except on the surface that does not explain the actual behavior in real-case scenarios.

The primary reason for failure focused on in the modeling was the slide body created in the frictional layer with a fully specified method. Analyses with a regular circular method were also executed since the pore pressure increase was insufficient. These can be seen in the appendix B. The initial factor of safety is likewise in both methods but the thing separating them is the behavior of safety factor versus time. The pattern in the circular method is constant and provides a realistic result while the fully specified one shows big differences each time step. This behavior could be explained by the fixed locations in the frictional layer and thus not showing the actual critical slice.

7.2 Economic and social consequences

A landslide is not just the collapse of soil. Its impact reverberates far beyond the physical event, especially when it strikes in urbanized, densely populated areas near our cities. Its consequences cover different aspects as in socially, economically and various other critical dimensions. Socially it disrupts communities, displaces families, and fractures the sense of safety and belonging. Depending on the scale and placement of a landslide it can result in loss of lives adding a tragic dimension to its impacts. Economically, the aftermath of a landslide entails significant costs to restore infrastructure damages, loss of property. More examples of this aspect are mentioned in the chapter regarding Stenungsund and the municipalities' measures concerning it. Dealing with the consequences of landslides demands a comprehensive approach that considers social, economic, environmental, health, cultural, and planning factors. This integrated approach builds resilience, reduces future risks, and enhances the welfare and sustainability of landslide-affected communities. Studies similar to this project and the gained knowledge from historical cases contribute to an enhanced geotechnical foundation and further understanding of effective mitigation strategies.

7.3 Learning from our mistakes and Urbanization's Impact

Although one would have wished to avoid the catastrophes that landslides bring, we believe they serve a purpose in promoting increased caution. Before the case of Tuve, there was a lack of documentation about quick clay and landslides. Since then several cases have provided us with specific knowledge while examining the main cause behind different landslides. The future holds numerous construction projects thus this knowledge together with the subsequent precautionary measures are necessary to minimize the risk of future landslides.

As discussed in the previous chapters of the report, a significant amount of the earlier landslides were deteriorated by extra strains from urbanization. As cities expand to accommodate growing populations, natural landscapes are often altered by deforestation, excavation, and construction. These alterations disrupt natural drainage patterns and increase runoff, leading to erosion and a heightened likelihood of slope failures.

Time-based erosion caused by urbanization can be triggered by minimal disturbance making the prediction and prevention of the event difficult, posing a significant challenge for the future. Landslides in Tuve and Gjerdrum serve as prime examples of this challenge. However, proactive measures can be taken to mitigate these risks. Implementing stricter land-use regulations, conducting thorough geological surveys before construction projects, and investing in robust slope stabilization techniques are essential steps in preventing future landslides. Additionally, advanced technologies such as satellite imaging and sensors can be used to enhance monitoring and early warning systems for potential landslides. In the case of the landslide in Stenungsund clear evidence of settlements in the area was provided by inSAR. These large settlement indicates that there is a mighty layer of clay and not bedrock as assumed in the geotechnical map of the area. The data from inSAR could have led to a reevaluation of the geology of the area and thus prompted further investigations to determine the true extent of the clay.

Despite the documentation of quick clay mapping and investigations, its effective utilization remains limited unless integrated into regulatory frameworks. To minimize future disasters, areas prone to quick clay should be thoroughly examined. Highly populated areas may require reinforcement measurements to follow future safety requirements. Improving terrain monitoring of erosion and other changes in the terrain can also be an example of practical applications to achieve desired outcomes taking quick clay seriously.

8 Final remarks

The discussion on landslides highlights the significant impact of global warming on slope stability and the occurrence of landslides. Changes in hydrology, particularly increased precipitation, can lead to critical conditions for slope failure due to higher flow and discharge, which erode banks and alter groundwater levels, affecting material stresses and shear strength. Additionally, increased seepage can amplify gravitational forces, potentially triggering slides. Engineering slopes may require reevaluation to cope with higher precipitation demands on drainage systems. Artesian pressure, resulting from confined groundwater under pressure, can uplift slopes and reduce frictional resistance, increasing landslide risk, particularly with increased precipitation.

In addition to natural forces, human activities have a significant part in the triggering factors. Urbanization and growing population require the use of land and can in different ways affect the natural elements. Decreased vegetation can consequently change the natural infiltration patterns, and constructions add additional load to the sensitive soil.

The complex interactions between climate change, human factors, and slope stability highlight the need for further research and monitoring for a better understanding and management of these risks.

References

[1] Karin Rankka et al. "Quick clay in Sweden". In: *Swedish Geotechnical Institute* 65 (2004), p. 148. URL: http://www.swedgeo.se/upload/publikationer/Rapporter/pdf/SGI-R65.pdf.

[2] Stig Bernander. "Progressive Landslides in Long Natural Slopes". PhD thesis. 2011. ISBN: 978-91-7439-283-8. URL: https://www.diva-portal.org/smash/get/diva2:990878/FULLTEXT01.pdf.

[3] Stefano Luigi Gariano and Fausto Guzzetti. *Landslides in a changing climate.* 2016. DOI: 10.1016/j.earscirev.2016.08.011.

[4] H Lee and J Romero. *Climate Change 2023 Synthesis Report IPCC.* Tech. rep. 2023, pp. 35–115. DOI: 10.59327/IPCC/AR6-9789291691647.

[5] IPCC. *Global Warming of 1.5°C.* Tech. rep. 2018. DOI: 10.1017/9781009157940.

[6] SGI. *Tuveskredet Geologi.* Tech. rep. Linköping: Statens geotekniska institut, 1981. URL: https://www.sgi.se/globalassets/publikationer/rapporter/pdf/sgi-r11b.pdf.

[7] Kristian Schoning. *Saltvattenavsatta leror i Sverige med potential för att bilda kvicklera.* Tech. rep. 2016. URL: https://www.sgu.se/globalassets/produkter/publikationer/tidigare/saltvattenavsatta-leror-i-sverige-med-potential-for-att-bilda-kvicklerasgu-rapport-2016-08.pdf.

[8] G. Thorsten B. Gunnar. *Tuveskredet, hydrogeologi.* Tech. rep. Linköping: Statens geotekniska institut, 1981. URL: https://sgi.se/globalassets/publikationer/rapporter/pdf/sgi-r11c.pdf.

[9] T Thorén, K Odén, and J Aradi. *PM Skred E6 Munkeröd, Stenungsunds kommun SGI:s TiB-insats, kvarvarande risker samt rekommendationer.* Tech. rep. Linköping: Statsens geotekniska institut, 2023, pp. 7–7. URL: www.sgi.se.

[10] Gösta Lundqvist. *Ba 18 Karta över landisens avsmältning och högsta kustlinjen i Sverige.* 1961. URL: https://apps.sgu.se/geolagret/GetMetaDataById?id=md-000919c5-2766-4143-9b07-154b07922d5e.

[11] Rolf Larsson. *Jords egenskaper.* swe. Tech. rep. Linköping, 2008, p. 58. URL: https://swedgeo.diva-portal.org/smash/get/diva2:1299902/FULLTEXT01.pdf.

[12] Karin Rankka. *Kvicklera - bildning och egenskaper. Litteraturstudie.* swe. Tech. rep. Linköping, 2003, p. 41. URL: https://www.diva-portal.org/smash/get/diva2:1300421/FULLTEXT01.pdf.

[13] Rolf Larsson. “Inverkan av förändringar i porvattnets kemi-främst salturlakning-på naturlig leras geotekniska egenskaper-Litteraturstudie”. In: (2010). URL: https://swedgeo.diva-portal.org/smash/get/diva2:1300503/FULLTEXT01.pdf.

[14] Roland Pusch. *Clay microstructure. A study of the microstructure of soft clays with special reference to their physical properties.* eng. Tech. rep. Stockholm, 1970, p. 76. URL: https://www.diva-portal.org/smash/get/diva2:1300152/FULLTEXT01.pdf.

[15] J. A. Knappett and R. F. Craig. *Craig's Soil Mechanics, Eighth edition.* 2012. DOI: 10.1201/b12841.

[16] Gunnar Beskow. *Om jordarternas kapillaritet : En ny metod för bestämning av kapillärkrafter (eller kapillära stighöjden).* swe. Tech. rep. Stockholm, 1930, p. 64. URL: https://resource.sgu.se/dokument/publikation/c/c356rapport/c356-rapport.pdf.

[17] Antonello Troncone et al. “A practical approach for predicting landslide retrogression and run-out distances in sensitive clays”. In: *Engineering Geology* 326 (Dec. 2023), p. 107313. ISSN: 0013-7952. DOI: 10.1016/J.ENGGEO.2023.107313.

[18] John J. Clague and D. (Doug) Stead. “Landslides : types, mechanisms and modeling”. In: (2012), p. 420.

[19] D.M. Cruden and D.J. Varnes. “Landslide types and processes”. In: *Special Report - National Research Council, Transportation Research Board* 247 (1996), pp. 36–75.

[20] Ariane Locat et al. “Progressive failures in eastern Canadian and Scandinavian sensitive clays”. In: (2011). DOI: 10.1139/T11-059. URL: www.nrcresearchpress.com/cgj.

[21] Stig Bernander. *Down-hill Progressive Landslides in Soft Clays.* Tech. rep. 2008. URL: https://www.diva-portal.org/smash/get/diva2:995262/FULLTEXT01.pdf.

[22] O N The and Lldan River. *THE LANDSLIDE AT SKOTTORP.* Tech. rep. 1946.

[23] Christoffer With et al. “A methodology for mapping of quick clay in Sweden”. In: *Natural Hazards* 112.3 (2022). ISSN: 15730840. DOI: 10.1007/s11069-022-05278-y.

[24] SGU. *Stora skred i Sverige.* 2024. URL: https://www.sgu.se/samhallsplanering/risker/skred-och-ras/stora-skred-i-sverige/.

[25] Jan Hartlén. *Tuveskredet slutrapport.* Tech. rep. Linköping: Statens geotekniska institut, 1984. URL: https://www.sgi.se/globalassets/publikationer/rapporter/pdf/sgi-r11a.pdf.

[26] SGI. *Metodik för kartläggning av kvicklera Vägledning SGI Publikation 46 Linköping 2018*. Tech. rep. Linköping: Statens geotekniska institut, 2018. URL: https://swedgeo.se/globalassets/publikationer/sgi-publikation/sgi-p46.pdf.

[27] SGI. *Tuveskredet 1977-11-30. Inlägg om skredets orsaker*. Tech. rep. Linköping: Statens geotekniska istitut, 1981. URL: https://www.sgi.se/globalassets/publikationer/rapporter/pdf/sgi-r10.pdf.

[28] SHK. *Jordskred vid vägbygge E6 i Småröd*. Tech. rep. Swedish Accident Investigation Board, 2009. URL: www.havkom.se.

[29] Trafikverket. *E6 förbi Stenungsund öppnas för trafik igen under 2024*. Feb. 2024. URL: https://www.trafikverket.se/om-oss/nyheter/nationella-nyheter/2024/februari/e6-forbi-stenungsund-oppnas-for-trafik-igen-under-2024/.

[30] Stenungsund kommun. *Frågor och svar om skredet 23 september*. Apr. 2024.

[31] SVT. *Nya dokument visar: Risker för skred vid E6 ströks ur handlingarna – Stenungsund godkände bygge utan nya mätningar*. Nov. 2023. URL: https://www.svt.se/nyheter/lokalt/vast/nya-dokument-visar-risker-for-skred-vid-e6-stroks-ur-handlingarna-stenungsund-godkande-bygge-utan-nya-matningar--54hto9.

[32] SVT. *Norconsult: Kompletterande undersökning behövdes innan bygge vid E6 i Stenungsund*. Feb. 2024. URL: https://www.svt.se/nyheter/lokalt/vast/norconsult-kompletterande-undersokning-behovdes-innan-bygge-vid-e6-i-stenungsund.

[33] Zetterlund Magnus. *Del av Munkeröd 1:12 m.fl. Stenungsund-detaljplan*. Tech. rep. URL: https://www.stenungsund.se/download/18.3d331977172708686c3e0b8/1591089621156/Hydrogelogi_Munker%C3%B6d%20PM.pdf.

[34] Stenungsund. *Del av Munkeröd 1:12 m.fl.* Tech. rep. URL: https://www.stenungsund.se/download/18.3d331977172708686c3e0bc/1591089621549/PM_Del%20av%20Munker%C3%B6d%201.12%20med%20flera.pdf.

[35] SVT. *Skredet på E6: Här är kartan som lurade experterna – före raset*. Feb. 2024. URL: https://www.svt.se/nyheter/lokalt/vast/skredet-pa-e6-har-ar-kartan-som-lurade-experterna-markerade-lera-som-berg.

[36] SVT. *Lerskredet vid Stenungsund – detta har hänt*. Mar. 2024.

[37] SVT. *Teorin: Tre gånger för mycket schaktmassor orsakade raset på E6 i Stenungsund*. Apr. 2024. URL: https://www.svt.se/nyheter/lokalt/vast/tre-misstanks-ha-orsakat-skredet-vid-e6-i-stenungsund-presskonferens-i-dag.

[38] Norwegian Geological Survey. *Gjerdrumskredet*. URL: https://www.ngu.no/geologi-og-risiko/gjerdrumskredet.

[39] Rapport fra ekspertutvalg. *Årsakene til kvikkleireskredet i Gjerdrum 2020*. Tech. rep. 2021. URL: https://www.regjeringen.no/contentassets/3dadc8f7fad94608861163fa524023c0/no/pdfs/arsakene-til-kvikkleireskredet-i-gjerdrum-2020.pdf.

[40] R.P. Allan et al. *Advances in understanding large-scale responses of the water cycle to climate change*. Vol. 1472. 1. 2020, pp. 49–75. DOI: 10.1111/nyas.14337.

[41] June-Yi Lee et al. *Climate: Scenario-Based Projections and NearTerm Information. In Climate Change 2021: The Physical Science Basis*. Tech. rep. 2021, pp. 553–672. DOI: 10.1017/9781009157896.006. URL: https://doi.org/10.1017/9781009157896.006.

[42] Piers Forster et al. *The Earth's Energy Budget, Climate Feedbacks, and Climate Sensitivity. In Climate Change 2021: The Physical Science Basis*. Tech. rep. 2021, pp. 923–1054. DOI: 10.1017/9781009157896.009. URL: https://doi.org/10.1017/9781009157896.009.

[43] R. Rajapakse. *Pile Design and Construction Rules of Thumb: Second Edition*. 2016, pp. 1–355. ISBN: 9780128042021. DOI: 10.1016/C2015-0-01495-2.

[44] J.H. Kim et al. "Vegetation as a driver of temporal variations in slope stability: The impact of hydrological processes". In: *Geophysical Research Letters* 44.10 (2017), pp. 4897–4907. DOI: 10.1002/2017GL073174.

[45] Göran Sällfors. *Geoteknik*. Cremona, 2013.

[46] Laxman Kafle et al. "A numerical investigation of slope stability influenced by the combined effects of reservoir water level fluctuations and precipitation: A case study of the Bianjiazhai landslide in China". In: *Engineering Geology* 297 (Feb. 2022). ISSN: 00137952. DOI: 10.1016/j.enggeo.2021.106508.

[47] Delwyn G. Fredlund, Harianto Rahardjo, and Murray D. Fredlund. *Unsaturated Soil Mechanics in Engineering Practice*. 2012. DOI: 10.1002/9781118280492.

[48] GEO-SLOPE. "Stability Modeling with GeoStudio". In: *GeoStudio* (2023). URL: https://downloads.geoslope.com/geostudioresources/books/11/2/SLOPE%20Modeling.pdf.

[49] Yoo Jae Kim et al. "Geosynthetic Reinforced Steep Slopes: Current Technology in the United States". In: *Applied Sciences 2019, Vol. 9, Page 2008* 9.10 (May 2019), p. 2008. ISSN: 2076-3417. DOI: 10.3390/APP9102008. URL: https://www.mdpi.com/2076-3417/9/10/2008.

[50] N.R. Morgenstern and V.E. Price. "The analysis of the stability of general slip surfaces". In: *Geotechnique* 15.1 (1965), pp. 79–93. DOI: 10.1680/geot.1965.15.1.79.

[51] Rymdstyrelsen. *InSAR Sweden*. URL: https://insar.rymdstyrelsen.se/.

[52] Magnus Karlsson and Lovisa Moritz. *Trafikverkets tekniska krav för geokonstruktioner TK Geo 13*. Tech. rep. Trafikverket, 2016. URL: https://trvdokument.trafikverket.se/fileHandler.ashx?typ=showdokument&id=46592c07-199a-4d8b-b417-d82362c9f806.

Appendices

A Parameters

A.1

Material	Hydraulic conductivity[m/s]	Source
Dry crust	10^{-5}	[25]
Clay	10^{-8}	[11]
Friction layer	10^{-5}	[25]
Bedrock	Assumed 10^{-20}	By Authors

Saturated Hydraulic conductivity Tuve

A.2

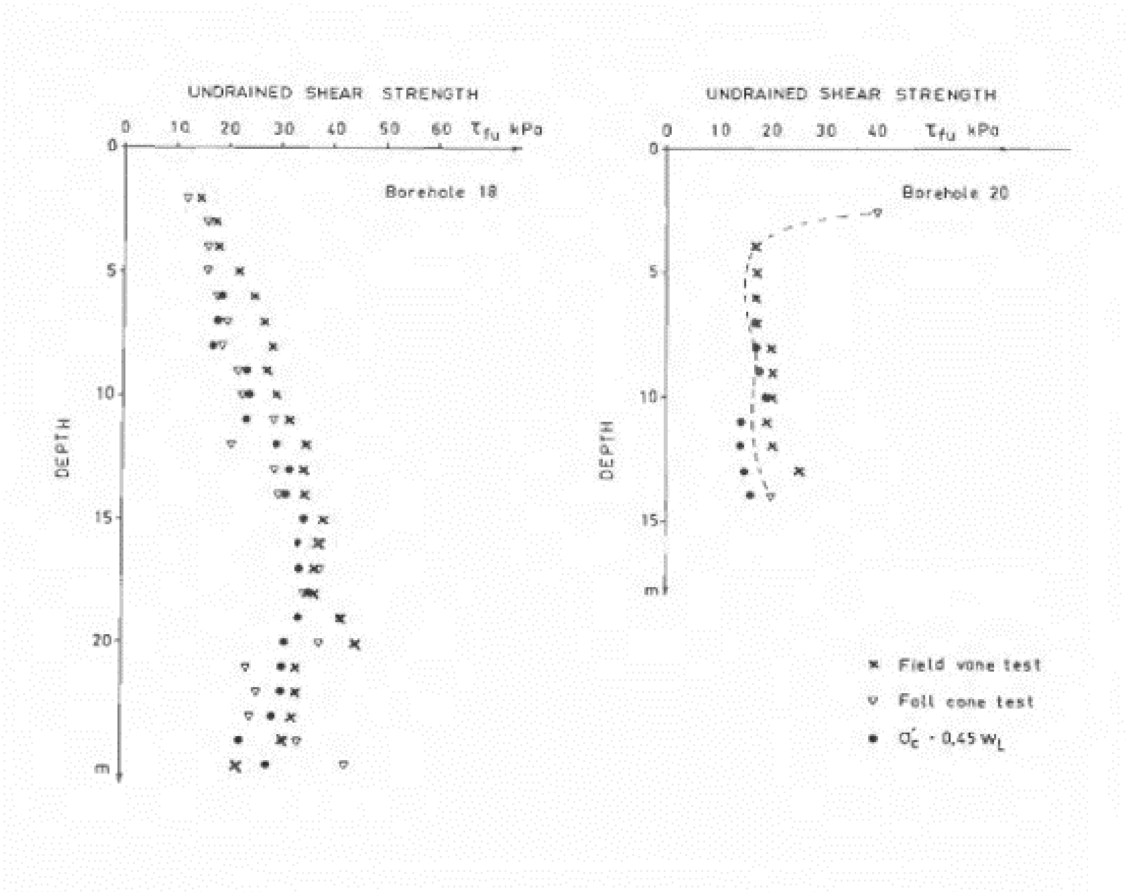

Shear strength parameters in borehole 18 and 19. [6]

A.3

Huvud-enhet	Nivå (cm u my	A n m ä r k n i n g
A	140-440	Gyttjelera. Grågrön. Homogen. Rikligt med växtrester. Enstaka stenar på nivå 430. Enstaka skal genom hela sektionen. Lerhalt varierande mellan ca 40-50 procent.
B	440-730	Finlera. Grå. Homogen. Växtrester förekommer ned till nivå 510. Enstaka skal genom hela sektionen. Mycket hög lerhalt (ca 70-75 %).
C	730-832	Mellanlera-Finlera. Grå. Kraftiga inslag av silt och sand i form av skikt eller linser, koncentrerade till nivåerna 770-790, 810-830. Sten på nivå 790. Enstaka skal samt ansamlingar av skal i vissa skikt. Lerhalt varierande mellan ca 35-60 %.
D	832-1120	Finlera. Grå. Homogen. Enstaka skal genom hela sektionen. Lerhalt varierande mellan ca 60-65 %.
	1120-1619	Finlera. Grå. Homogen. Ett tunt siltskikt på nivå 1413. Sten på nivå 1390. Enstaka skal genom hela sektionen. Fläckar och band av sulfider. Lerhalt varierande mellan ca 65-70 %.
	1619-1890	Finlera. Grågrön. Homogen. Enstaka skal genom hela sektionen. Lerhalt varierande kring 65 %.
	1890-2300	Finlera. Grågrön. Enstaka tunna siltskikt. Mörka band mellan nivåerna 2165-2170, 2200-2212, 2274-2279. Störningar mellan nivåerna 2255-2271. Enstaka skal genom hela sektionen. Lerhalt varierande mellan ca 55-60 %.
E	2300-2650	Grovlera-Finlera. Grågrön. Kraftiga inslag av silt och sand i form av skikt. Sten på nivå 2517. Störningar mellan nivåerna 2325-2334. Alternerande mörka och ljusa band. Enstaka skal ned till nivå 2412. Lerhalten mycket varierande (mellan ca 17-45 %).

Soil layer in borehole 18 [6]

A.4

Huvud-enhet	Nivå (cm u my)	Anmärkning
A	130-140	Mellanlera. Rödbrun. Kraftigt inslag av sand- och gruspartiklar, massformigt fördelade. Rikligt med växtrester. Lerhalt ca 35 %.
B	140-240	Finlera. Rödbrun. Visst inslag av silt och sand, men ej som skikt. Rikligt med växtrester. Lerhalt ca 60 %.
C	240-360	Finlera. Grågrön. Kraftiga inslag av silt och sand i form av skikt eller linser. Växtrester förekommer ned till nivå 350. Enstaka skal genom hela sektionen. Lerhalt varierande mellan ca 55-65 %.
D	360-970	Finlera. Grågrön. Homogen. Enstaka siltskikt på nivåerna 591, 742, 925 samt små spridda siltlinser. Enstaka skal genom hela sektionen. Ansamlingar av skal i anslutning till vissa linser. Lerhalt ca 60 %.
	970-1050	Finlera. Grågrön. Homogen. Sulfidbandning. Lerhalt varierande mellan ca 40-45 %.
	1050-1120	Finlera. Grågrön. Enstaka silt- och sandskikt. Sulfidbandning. Enstaka skal samt ansamlingar av skal i vissa skikt. Lerhalt ca 45 %.
E	1120-1400	Grovlera-Finlera. Gråbrun. Kraftiga inslag av silt och sand, i form av skikt eller linser. Alternerande mörka och ljusa band. Sten på nivåerna 1144, 1289. Skal förekommer ned till nivå 1330. Lerhalten varierande mellan ca 15-60 %.

Soil layers in borehole 20 [6]

B Results from Geostudio

B.1

Color	Name	Model	Unit Weight (kN/m³)	Cohesion' (kPa)	Phi' (°)	C-Top of Layer (kPa)	C-Rate of Change ((kN/m²)/m)	Cu-Top of Layer (kPa)	Cu-Rate of Change ((kN/m²)/m)
	Berg	Bedrock (Impenetrable)							
	Friktionslager	Mohr-Coulomb	17	0	30				
	Lera1	Combined, S=f(depth)	16		30	1.5	0.15	20	0.5
	Lera2	Combined, S=f(depth)	16		30	1.5	0.15	30	-0.5
	Torrskorpa	Mohr-Coulomb	15	0	30				

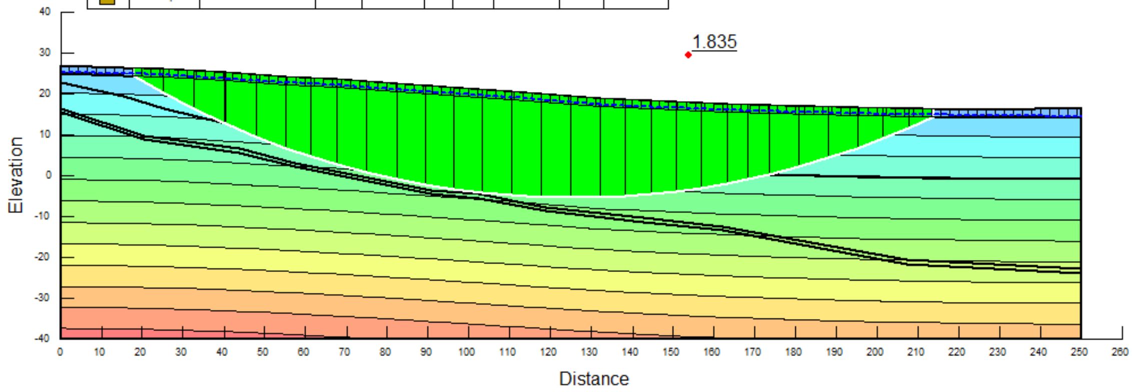

Circular slip surface in section A-A

B.2

Color	Name	Model	Unit Weight (kN/m³)	Cohesion' (kPa)	Phi' (°)	C-Top of Layer (kPa)	C-Rate of Change ((kN/m²)/m)	Cu-Top of Layer (kPa)	Cu-Rate of Change ((kN/m²)/m)
	Berg	Bedrock (Impenetrable)							
	Friktionslager	Mohr-Coulomb	17	0	30				
	Lera1	Combined, S=f(depth)	16		30	1.5	0.15	20	0.5
	Lera2	Combined, S=f(depth)	16		30	1.5	0.15	30	-0.5
	Torrskorpa	Mohr-Coulomb	15	0	30				

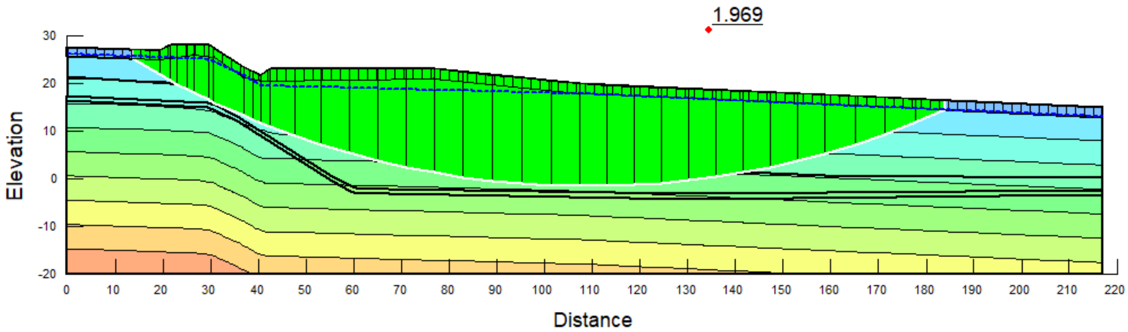

Circular slip surface in section B-B

B.3

Color	Name	Model	Unit Weight (kN/m³)	Cohesion' (kPa)	Phi' (°)	C-Top of Layer (kPa)	C-Rate of Change ((kN/m²)/m)	Cu-Top of Layer (kPa)	Cu-Rate of Change ((kN/m²)/m)
	Berg	Bedrock (Impenetrable)							
	friktionslager	Mohr-Coulomb	17	0	30				
	Lera 1	Combined, S=f(depth)	16		30	1.5	0.15	20	0.5
	Lera2	Combined, S=f(depth)	16		30	1.5	0.15	30	-0.5
	Torrskorpa	Mohr-Coulomb	15	0	30				

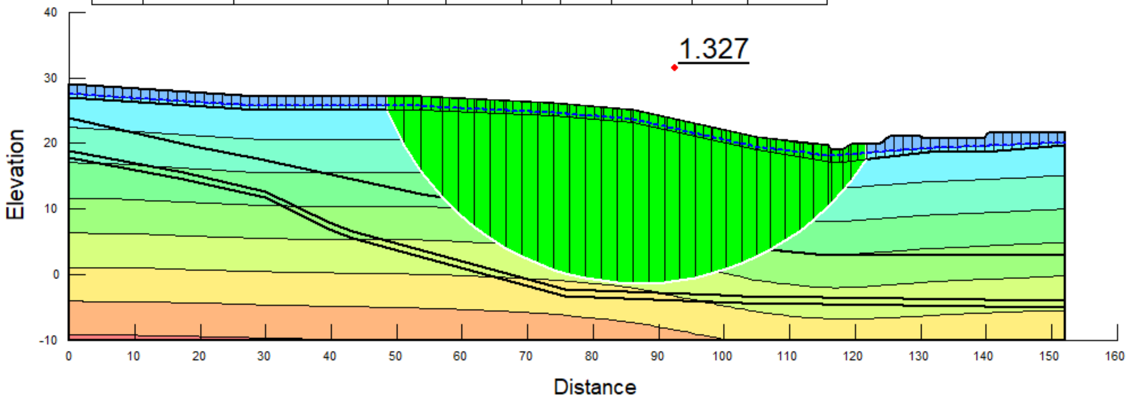

Circular slip surface in section C-C

B.4

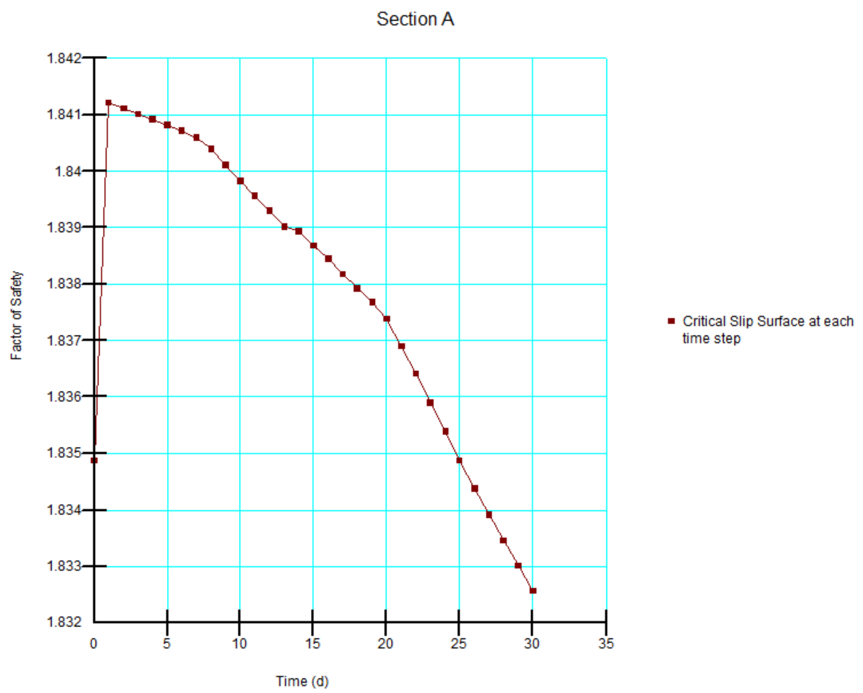

Factor of safety in section A-A

B.5

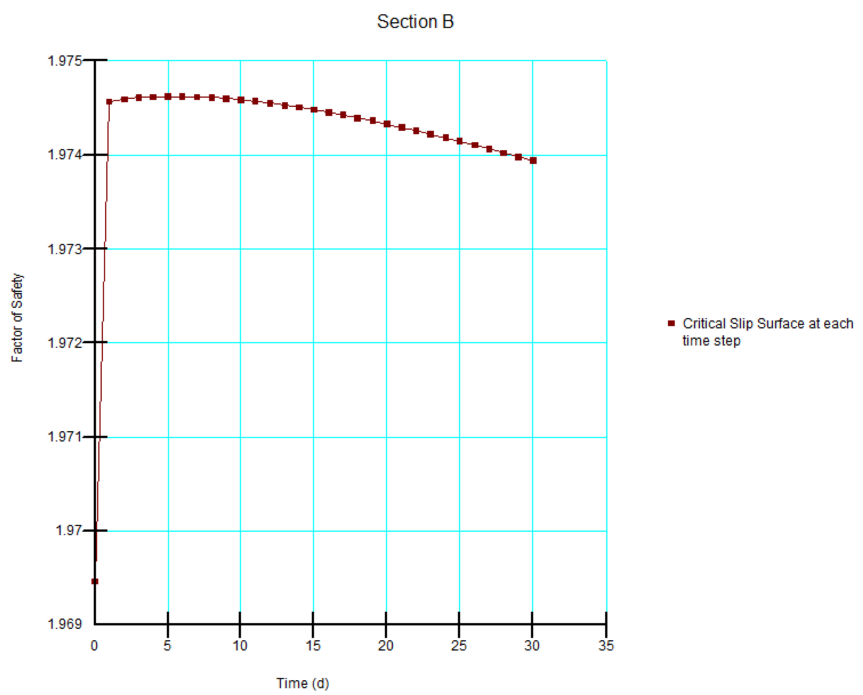

Factor of safety in section B-B

B.6

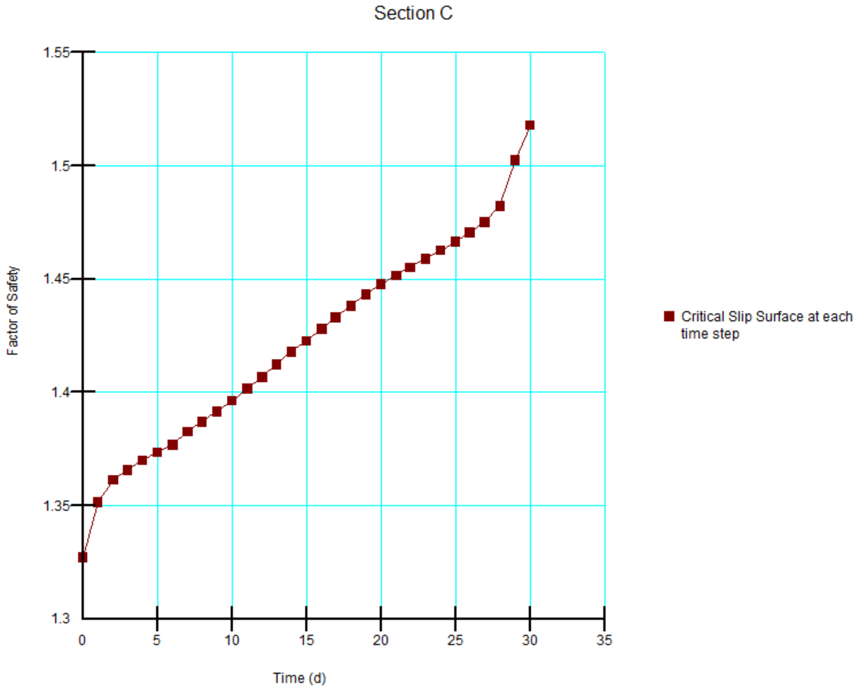

Factor of safety in section C-C

C Functions in Geostudio

C.1

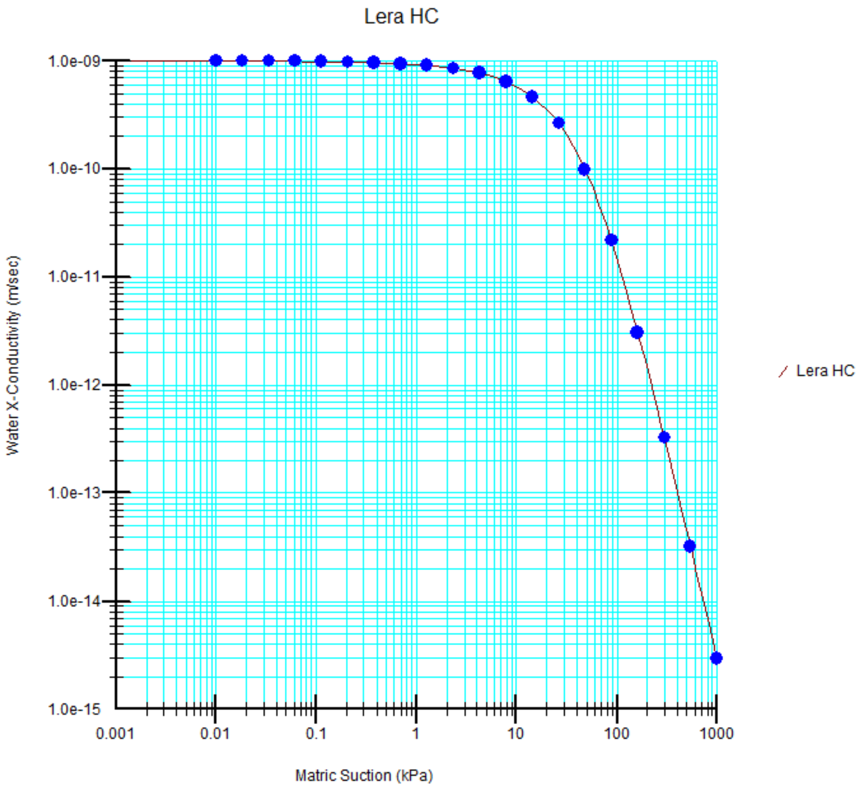

Water conductivity and matric suction, clay

C.2

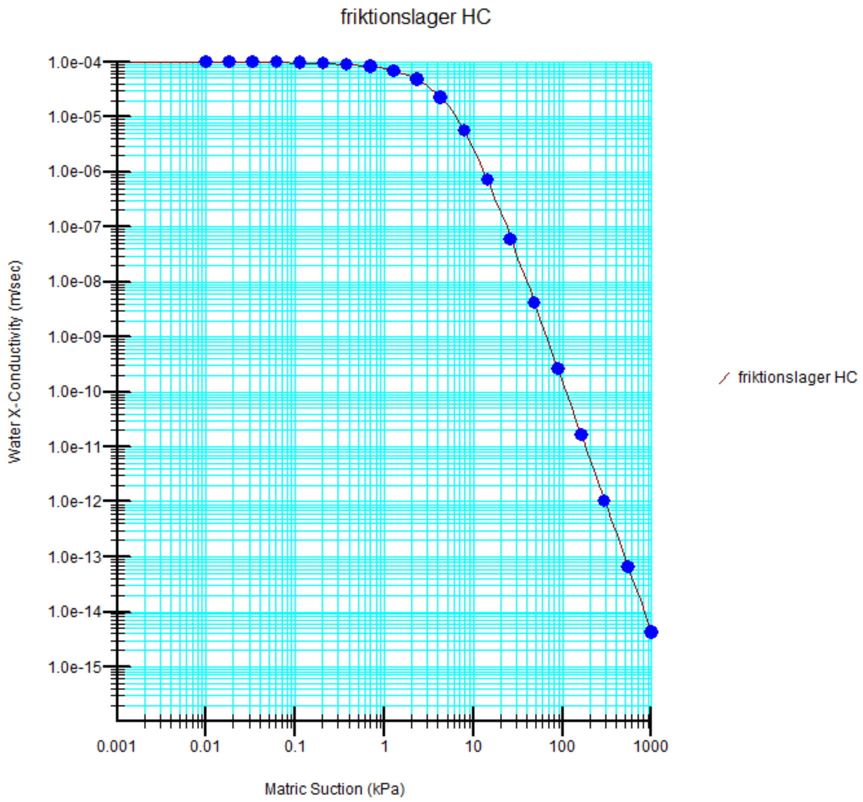

Water conductivity and matric suction, frictional layer

C.3

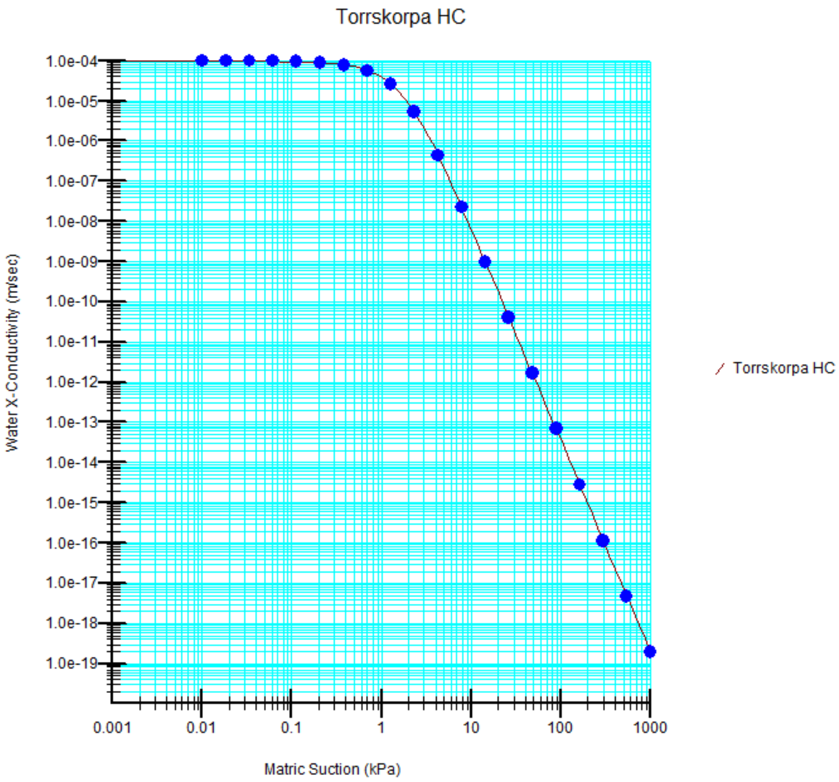

Hydraulic conductivity and matric suction, dry crust

C.4

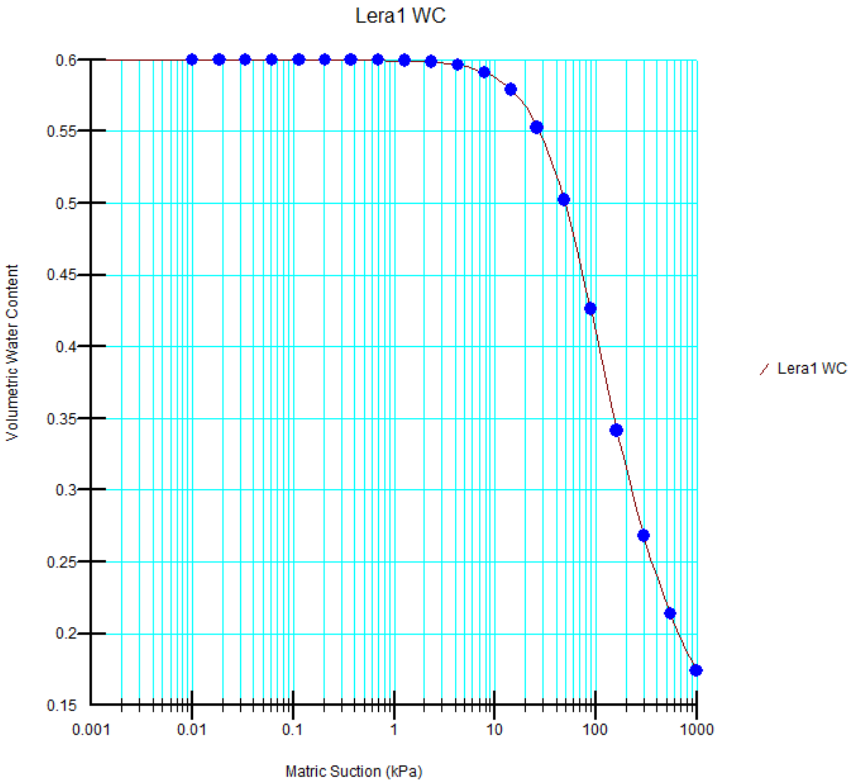

Volumetric water content and matric suction, clay 1

C.5

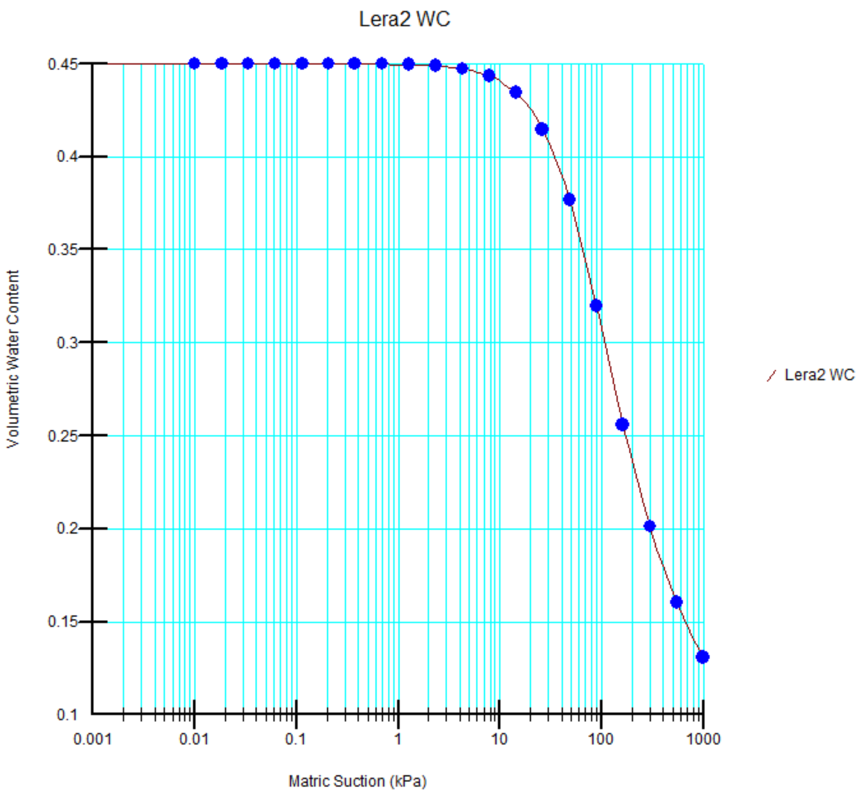

Volumetric water content and matric suction, clay 2

C.6

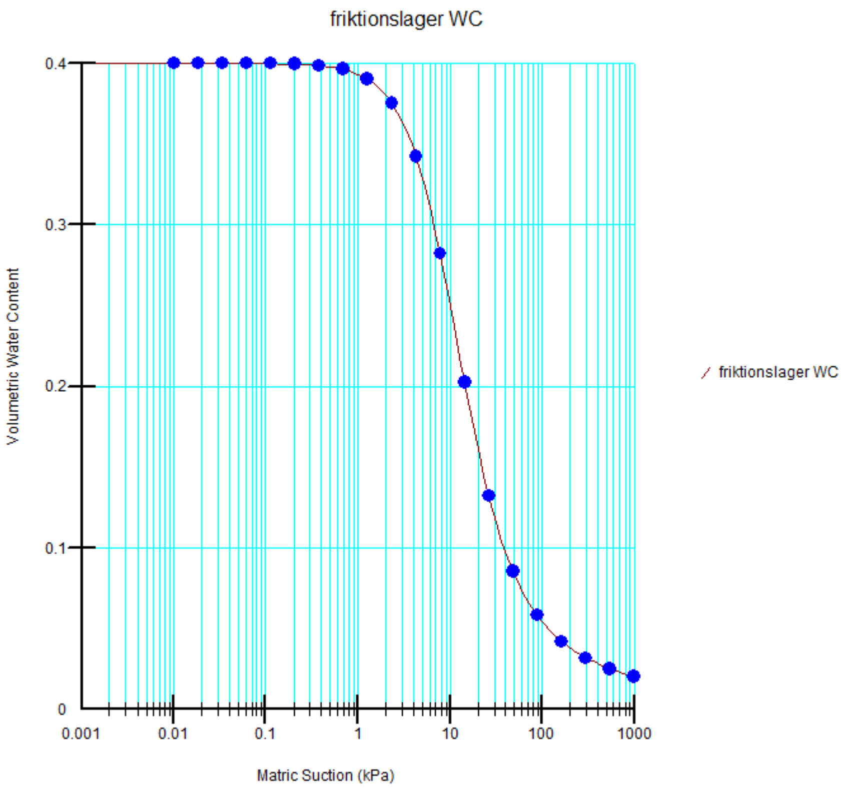

Volumetric water content and matric suction, frictional layer

C.7

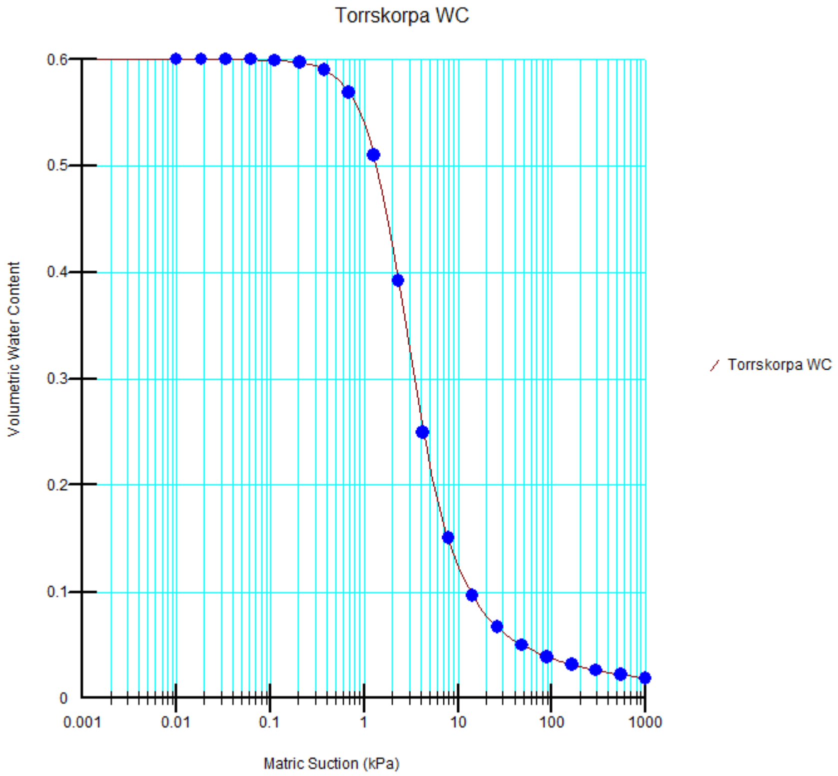

Volumetric water content and matric suction, dry crust